Biomedicine & Pharmacotherapy 200 (2026) 119578

Contents lists available at ScienceDirect

Biomedicine & Pharmacotherapy

journal homepage: www.elsevier.com/locate/biopha

Prevention of NMDA receptor sensitization by neurotoxic β-amyloid through polyphosphate coacervation

Werner E.G. Müller [a,*], Sanja Perovic-Ottstadt [a], Rita Dobmeyer [b], Meik Neufurth [a], Hadrian Nassabi [c], Rafael Muñoz-Espí [d], Hiroshi Ushijima [e], Heinz C. Schröder [a], Xiaohong Wang [a,*]

[a] ERC Advanced Investigator Grant Research Group at the Institute for Physiological Chemistry, University Medical Center of the Johannes Gutenberg University, Mainz 55128, Germany
[b] Galenus GH AG, Hergiswil 6052, Switzerland
[c] Clinic for Skin Diseases with Plastic Surgery SRH Wald-Klinikum Gera, Gera 07548, Germany
[d] Institute of Materials Science (ICMUV), Universitat de València, Paterna, València 46980, Spain
[e] Division of Microbiology, Department of Pathology and Microbiology, Nihon University-School of Medicine, Tokyo 173-2610, Japan

ARTICLE INFO

Keywords:
Inorganic polyphosphate
Serotonin
Coacervate
Neurotoxic effect
Alzheimer amyloid β peptide
NMDA receptor
Apoptosis
Calcium
Primary rat neuronal cells
Rat pheochromocytoma PC12 cells

ABSTRACT

Alzheimer's disease is characterized by amyloid-β (Aβ)–induced synaptic dysfunction and *N*-methyl-D-aspartate (NMDA) receptor–dependent calcium dysregulation, and inorganic polyphosphate (polyP), a platelet-enriched polymer released upon platelet activation, has emerged as a potential modulator of neuronal survival. Primary rat neuronal cultures and PC12 pheochromocytoma cells were exposed to the neurotoxic Aβ fragment Aβ (25–35), following a 2–5 day pre-incubation to induce its toxic conformation; neuronal apoptosis, NMDA receptor–mediated calcium influx, and the mechanistic basis of polyP action were assessed in the presence of sodium polyphosphate (Na-polyP), including experiments with calcium-chelating polyP coacervates formed in combination with serotonin, and the release kinetics of three polyP-based brain-targeted formulations were characterized. Pre-incubated Aβ(25–35) at 10 μM induced apoptotic neuronal death within 3 days, whereas coincubation with Na-polyP (50 μg/mL) abolished Aβ-induced neurotoxicity and significantly attenuated glutamate-evoked NMDA receptor–dependent calcium influx; mechanistic analyses demonstrated that Na-polyP forms calcium-chelating coacervates, promoted by serotonin at physiological Ca^{2+} concentrations, and that polyP nanogels, nanoparticles and micelle-based formulations exhibit controlled release profiles. These data identify calcium chelation *via* polyP coacervate formation as a key mechanism underlying protection against Aβ-induced NMDA receptor sensitization and neuronal death, and suggest that polyP-based strategies may provide a mechanistically grounded approach for therapeutic intervention in Alzheimer's disease.

1. Introduction

Calcium ions (Ca^{2+}) play a crucial role as second messengers in the body's metabolism, for example in muscle contraction [1], as a signaling molecule for hormone and enzyme secretion [2], and in triggering processes involved in cell proliferation and apoptosis [3]. In neuronal cells, Ca^{2+} ions regulate the release of neurotransmitters from the presynaptic terminals, which subsequently act on the postsynaptic neuron [4,5].

During aging, and especially in neurodegenerative disorders, Ca^{2+} regulatory circuits become dysregulated, leading to impaired plasticity and neuronal degeneration [6]. The critical step of Ca^{2+} influx into neurons is both voltage-dependent and dependent on ligand-gated channels inserted into the plasma membrane [7]. Among these ligands, glutamate, as important excitatory neurotransmitter in the central nervous system, induces an increase in cytoplasmic Ca^{2+} concentration by acting directly on the α-amino-3--hydroxy-5-methyl-4-isoxazole propionic acid (AMPA) and *N*-methyl--D-aspartate (NMDA) receptors and also indirectly by activating the voltage-dependent Ca^{2+} channels [8–12]. The neurotoxic effects

* Correspondence to: ERC Advanced Investigator Grant Research Group at the Institute for Physiological Chemistry, University Medical Center of the Johannes Gutenberg University, Duesbergweg 6, Mainz D-55128, Germany.
E-mail addresses: wmueller@uni-mainz.de (W.E.G. Müller), wang013@uni-mainz.de (X. Wang).

https://doi.org/10.1016/j.biopha.2026.119578
Received 18 March 2026; Received in revised form 11 May 2026; Accepted 21 May 2026
Available online 11 June 2026

caused by the rise in Ca^{2+} ions are due to the activation of cysteine proteases and caspases, leading to apoptosis [13,14], and the generation of oxidative radicals [15], as well as the increase in the concentration of calpain, which activates caspases [14].

Knowing that Ca^{2+} plays a crucial role in Ca^{2+}-induced neurotoxicity, our group discovered that the drug memantine, an NMDA receptor channel blocker [16], prevents the apoptotic collapse of neurons induced by the human immunodeficiency virus type 1 (HIV-l) coat protein gp120 [17,18]. This neuroprotective effect was confirmed by the group of Lipton [19]. A disturbed intracellular Ca^{2+} metabolism, caused by an increased influx of calcium ions *via* the NMDA receptor, also leads to neurological disorders such as Alzheimer's disease [20], and Parkinson's disease, caused by α-synuclein aggregation [21], as well as stroke, also caused by dysregulation of the NMDA receptor activity [6, 22]. The intracellular Ca^{2+} concentration in neurons is about 100 nM and can reach 1 mM and more in the signaling state after activation of the NMDA receptor [23,24]. Maiolino et al [25] described that the inorganic polymer polyphosphate (polyP) reduces glutamate-induced, and especially AMPA-induced, Ca^{2+} signalling; the effect with NMDA is slightly lower. They also showed that there are $P2Y_1$ receptors that are stimulated by the polymer [26]. Based on their data, they concluded that polyP is protective against Ca^{2+} dysregulation and glutamate excitotoxicity.

As recently outlined [27], the aging process, particularly neuronal aging, which increases the risk of various neurological, especially neurodegenerative, diseases, is closely linked to energy homeostasis. Therefore, it is conceivable that the mitochondria, as the main energy factories of brain cells, must precisely adapt to the energy demand of synaptic activity [28].

Alzheimer's disease is a progressive neurodegenerative disorder commonly associated with memory deficits and cognitive decline [29]. The aggregates in Alzheimer's disease originally described as colloidal deposits [30] were later named amyloid deposits, or, more specifically, amyloid β (Aβ)-protein deposits [31]; these authors also concluded from their findings that the Aβ-deposits, which are found in both senile plaques and blood vessels, are distributed R*via* the blood vessels into the white matter of brains affected by Alzheimer's disease. The toxic Aβ deposits originate after sequential proteolysis from a single-pass transmembrane protein, the amyloid precursor protein (APP) [32]. Particularly interestingly, APP is also formed in the platelets and processed by the hydrolytic enzymes β- and γ-secretase [33,34]. The resulting Aβ peptides further aggregate into amyloid plaques composed of Aβ and neurofibrillary tangles, which in turn are assembled from hyper-phosphorylated tau proteins [35]. The natural Aβ42 and Aβ40 monomers are either randomly coiled or form an α-helix. During this transition, the natural structure transforms into a β-sheet (reviewed in: ref [36]), and the oligomers interact with the

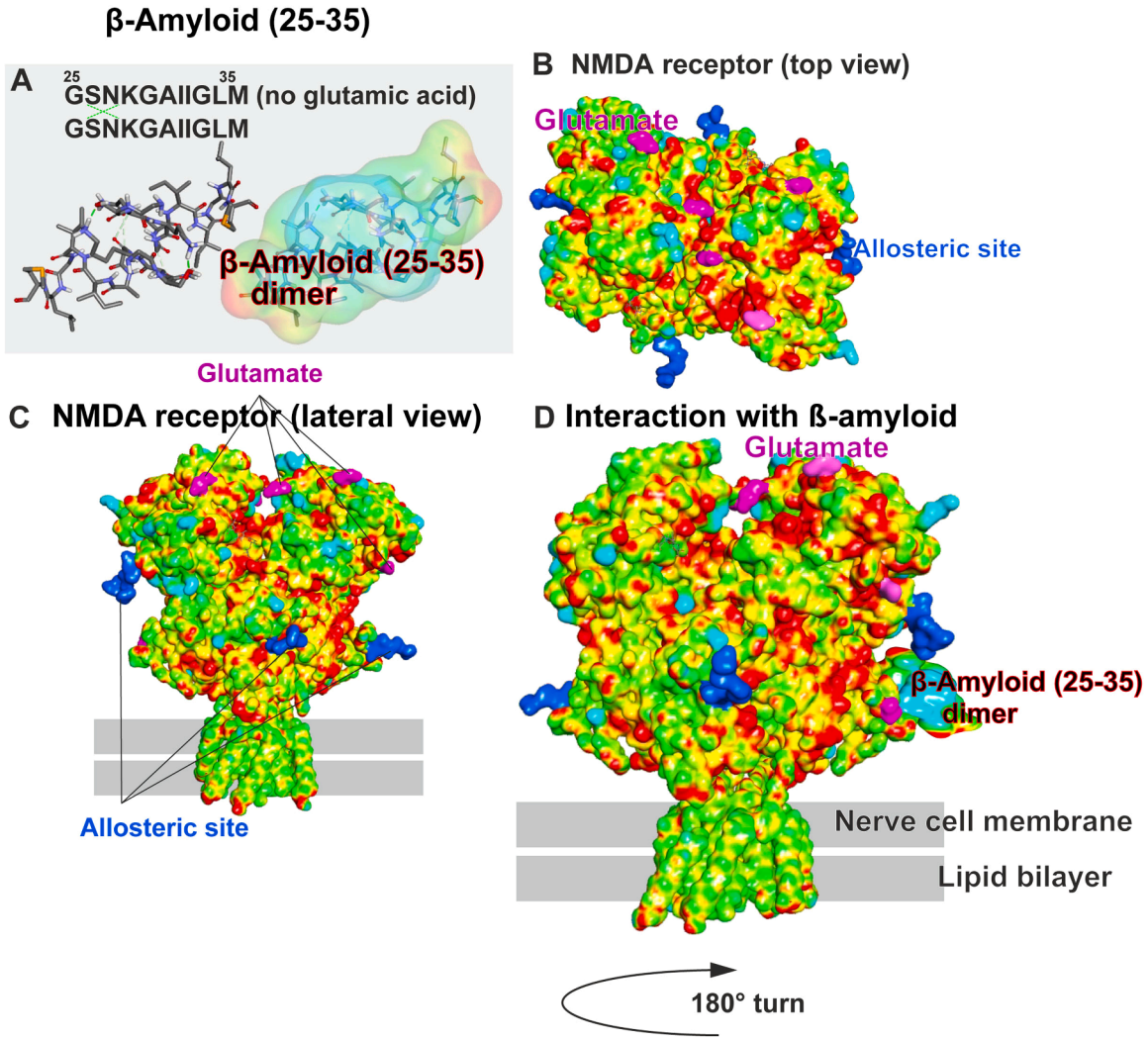

Fig. 1. Structure and interaction of β-amyloid with the NMDA receptor. (A) Model of the neurotoxic β-amyloid (Aβ(25−35)) dimer (left) and its surface charge/ribbon structure (shown in transparency) (right). (B) Top view and (C) lateral view of the NMDA receptor. The allosteric site and the Glu residues (in magenta) are marked. (D) Interaction of the neurotoxic β-amyloid dimer with the GluN2B subunit of the NMDA receptor.

synaptic NMDA receptor [37], a process in which the tau protein is involved *via* the CAMKK2-AMPK kinase [38]. Certainly, the three glutamate residues protruding from Aβ and its ribbon play a functional role in the synaptic toxicity of Aβ. However, for the studies conducted here, the Aβ(25−35) fragment was used, which contains no glutamic acid residues (Fig. 1A). This fragment is also neurotoxic due to induction of apoptosis, as shown later and described before [39,40]. Strong evidence has been presented that the amyloid-β oligomers bind to the NMDA receptor at its metabotropic glutamate receptor 2/3 (mGluR2/3) subunit at the glutamate binding site, to which also NMDA binds [41]. The fact that the Aβ (25−35) peptide NH_2-Gly-Ser-Asn-Lys-Gly-Ala-Ile-Ile-Gly-Leu-Met-COOH does not comprise a glutamic acid residue supports the assumption that the NMDA receptor interacts with the Aβ peptide(s) *via* its allosterically regulatable site (Fig. 1B to D); this site is predicted to be located close to the laterally oriented glutamate entities [41].

As summarized [42], experimental data suggested that the toxic oligomers from Aβ are more relevant than plaques with respect to the cognitive decline. It has been originally described that Aβ is responsible for the neurotoxicity to neuronal cells [43]. Shortly later, it was reported that the Aβ(1−40) increases the vulnerability of neurons to excitotoxins such as glutamate and NMDA [44]. Then, it was found that the neurons undergo apoptosis as revealed by scanning electron microscopy (SEM) [45]. Our group presented the clear DNA fragmentation pattern as further evidence for the apoptotic degradation of neuronal DNA [46].

It has been proposed that the platelets are "circulating mirrors of neurons" because a series of proteins is expressed in both cell types [47]. The platelets also contain the highest level of polyP, a polymer that is basically present in all metazoan cells [48]. PolyP acts as a cell signaling molecule and induces regeneration in organs without a dense blood vessel supply [49]; this is particularly evident in wound healing [48,50,51]; in this area of application, the regenerative effect of polyP has been clinically demonstrated due to enhanced fibrin clotting and the recruitment of fibroblasts and their differentiation into myofibroblasts.

PolyP is physiologically formed in the precursor cells of the platelets, the megakaryocytes, and there in the vicinity of the mitochondria, most likely *via* the F_oF_1-ATP synthase [52] (reviewed in ref [53]). This polymer represents the body's densest metabolically usable energy source, as its phosphate (P_i) units are linked linearly up to 1000 units *via* high-energy phosphoric anhydride bonds. The metabolic energy stored in polyP is regained during enzymatic degradation of the polymer by the combined action of cell membrane-associated alkaline phosphatase (ALP) and adenylate kinase (ADK) [53]. This energy can then be used to sustainably and long-lastingly support any regeneration process in the body. This was successfully documented in a proof-of-concept study with patients suffering from chronic wounds [50,51]. The chain length of the polyP molecules can reach 1000 P_i units in bacteria. In contrast, their length is much shorter in mammalian systems, with only 60 −100 P_i units [54–56]. It has been published that polyP is released from the platelet dense granules both as free polyP and as particle-associated Ca-polyP. Ca^{2+} is a major ion in those granules. In the presence of Ca^{2+} in the extracellular space at the sites where polyP is released from the platelets, the polymer undergoes a coacervation process [57,58].

At present, based on the existing data, there are three main approaches that could prevent Aβ-elicited neurotoxicity. First, down-regulation of Aβ production by inhibiting/modulating secretase activity [59]. Second, prevention of Aβ plaque formation. In this context, it has been published that polyP, applied as Na-polyP [60], serves as an effective nucleation source for a series of different amyloid proteins, including Aβ(1–40/42). In contrast, it has been experimentally shown that, in worm *Caenorhabditis elegans*, polyP even protects cells from the toxic effects of amyloids. While polyP accelerates nucleation and fibril formation, it simultaneously reduces the number of toxic oligomers required for fibril formation. Third, elimination/balancing of the rise of Ca^{2+} around the NMDA receptor. The extracellular Ca^{2+} level in the cerebrospinal fluid is ≈ 1 mM [61]. The addition of ethylene glycol bis (2-aminoethyl ether)-*N*,*N*,*N*′,*N*′-tetraacetic acid (EGTA), a specific Ca^{2+} chelating agent in the extracellular space, blocks NMDA-induced Ca^{2+} influx into neurons [62]. Or, fourth, feeding of postulated extracellular chaperones with ATP-generating polyP [63].

In the present contribution, we document the effect of polyP as a protective polymer against Aβ-induced apoptosis in fetal rat primary neurons. The cells were prepared from 19-day-old Wistar rat embryos, as these have the highest density of NMDA receptors [64]. They were treated with Na-polyP, which undergoes coacervation in the presence of Ca^{2+} [57]. PolyP occurs both intracellularly [65] and extracellularly, as it reaches the injured region *via* the platelets. However, for medical translation, Na-polyP must pass the blood-brain barrier, a complex structure, which is stabilized by the vascular endothelial cells. These cells, with their homeostatic processes, are connected by tight junctions, allowing only a very restricted passage of metabolites across the barrier. This barrier also enables the transport of polar substances, such as, presumably, polyP [66]. Also liposomes/micelles can cross the barrier [67,68].

The intranasal route has been described as an attractive and alternative, non-invasive route for targeted delivery of therapeutics to the brain, because it allows bypassing the blood-brain barrier and the problems associated with uptake *via* the gastrointestinal tract [69,70]. However, this route also requires a suitable transport vehicle.

Therefore, this contribution also describes the preparation of three vehicles proposed for targeted delivery of polyP to the brain. First, a stabilized polyP nanogel enabling the transport *via* the coacervate phase [71]. At a slightly higher pH, nanoparticles are formed that also allow the transport of the polymer to the target site [72]. Finally, polyP-loaded nanoparticle-micelles were fabricated, which have proven to be effective vehicles for crossing the blood-brain barrier. To deliver Na-polyP *via* a nasal spray, a formulation suitable for targeted brain delivery was developed.

2. Materials and methods

2.1. Materials

The toxic amyloid β-protein fragment 25–35 was purchased from Sigma-Aldrich (#A4559; Taufkirchen; Germany). To convert the inactive peptide, termed Aβ(25−35)-i, into the active, toxic form, a stock sample in distilled water (900 μM) was prepared and stored at 4°C for 5 days (or, if indicated, 2 or 3 days) prior to use [46]. This preparation was designated Aβ(25−35)-a. Unless otherwise stated, the respective sample was added at a concentration of 10 μM (M_r: 1060; 10.6 μg/mL).

For comparison, the amyloid-β-protein fragment 1–42 (#A9810; Sigma-Aldrich) was used in some experiments. The peptide was reconstituted in ammonium hydroxide pH > 9 [73], according to the instructions from the manufacturer. The resulting stock solution (1 mg/mL) was then serially diluted in PBS and finally in distilled water to obtain the active, neurotoxic form (named Aβ(1−42)-a), which was also used at a concentration of 10 μM (M_r: 4514; 45.1 μg/mL).

2.2. Preparation of Na-polyP

The polymer was prepared from sodium-phosphate (NaH_2PO_4; #S5011; Sigma-Aldrich) by polymerization at 750°C in a muffle furnace for 4 h, followed by rapid cooling [74].

2.3. Protein modelling

The models of the Aβ(25−35)-amyloid and for the NMDA receptor were taken from the PDB-Protein Data bank. All molecular graphics and amino acid analyses were performed either with the Discovery Studio Visualizer (Dassault Systèmes) [75] powered by the UCSF Chimera version 1.14. For each protein-protein association, at least 300 cleaning cycles were applied.

2.4. PolyP-based coacervate formation in cerebrospinal fluid

According to the determined physiological concentrations, the artificial cerebrospinal fluid used contained 124.2 mM NaCl, 2.79 mM KCl, 1.14 mM $MgCl_2$, 23 mM $NaHCO_3$, 0.4 mM NaH_2PO_4, 1.18 mM $CaCl_2$, and 3.66 mM D-glucose [61]. The pH was adjusted to 7.3.

To promote coacervate formation of the polyanionic polyP and to stabilize the coacervate, we added serotonin (serotonin hydrochloride; #H9523; Sigma-Aldrich) as a cationic component at the pH of 7.0 chosen [76]; this even allows oligomerization of the neurotransmitter [77]. This biogenic amine is a tissue hormone that, together with NMDA receptors in the prefrontal cortex, is involved in the regulation of cognition and emotion under normal and pathological conditions [78].

The final concentrations in the coacervate were chosen at 47 mM serotonin (if selected), 1.18 mM $CaCl_2 \bullet 2H_2O$ (#C8106; Sigma-Aldrich) and, where indicated, 39 mM Na-polyP (4 mg/mL).

2.5. Isolation and cultivation of primary neuronal cells

The cells were obtained from the brains of 17- to 18-day-old Wistar rat embryos, according to the described method [79]. In short, brain tissue was dissociated with 0.025% trypsin in Hanks' balanced salt solution [1:10 dilution from SM-2003-C (Sigma-Aldrich) without Ca^{2+} and Mg^{2+}]. After centrifugation, the cells were resuspended in Dulbecco's modified Eagle's medium (4500 mg glucose/L; DMEM/HG) (#D6429, Sigma-Aldrich) serum-free enriched with 0.1% (w/v) bovine serum albumin (BSA), 100 mU/L insulin, 2 mM L-glutamine, 100 μg/mL transferrin, 16 μg/mL putrescine, 6.3 ng/mL progesterone, and 5.2 ng/mL Na_2SeO_3. To increase the yield of neurons, the suspension was treated with medium containing 10 μM uridine, 10 μM fluoro-deoxyuridine, and 1 μM cytosine arabinofuranoside (to eliminate proliferating non-neuronal cells) for 3 days. Immunostaining with anti-68-kDa neurofilament as a marker for neurons and anti-glial fibrillary acidic protein for glial cells indicated that the cultures contained > 85% neurons.

Where indicated, the neuronal cultures were incubated with 50 μg/mL of Na-polyP in the presence or absence of Aβ(25−35)-a or Aβ(1−42)-a at the concentrations indicated with the results.

In one series of experiments, neuronal PC12 cells (rat pheochromocytoma cells; #88022401, from Sigma-Aldrich) were used. The cells were cultivated in DMEM medium (Sigma-Aldrich) and heat-inactivated horse serum (5%)/heat-inactivated fetal bovine serum (10%), together with gentamicin as described [63]. After overnight pre-incubation, the cells were overlaid with a polyP-based coacervate formed by addition of 100 μL of 47 mM serotonin and 1.18 mM $CaCl_2$ together with Na-polyP (final concentration 4 mg/mL). The cultures were then incubated for 0–72 h.

2.6. Assessment and quantification of apoptosis

Apoptosis was determined using the DNA fragmentation assay [80]. After DNA extraction, the material was size separated by electrophoresis [80] and processed for UV fluorescence visualization by staining with ethidium bromide [17].

For quantification, the Cell Death Detection ELISAplus kit (Cat. No. 11 774 425 001, Roche) was used as previously described [81]. This photometric enzyme immunoassay measures apoptosis by quantifying cytoplasmic histone-associated DNA fragments. Measurements were performed at 405 nm against substrate solution as a blank. The background values (incubation buffer instead of sample solution) were subtracted.

2.7. Determination of cell viability

Cell viability was determined using the colorimetric MTT assay (3-[4,5-dimethylthiazol-2-yl]-2,5-diphenyltetrazolium bromide; #CT01, Sigma). After color development of the insoluble formazan product, the plates were read at 570 nm using an ELISA reader.

2.8. Determination of intracellular Ca^{2+} concentration

For these experiments, we followed the described procedure [8,82]. Neuronal cells cultivated on poly-L-lysine coated borosilicate coverslips (Nunc, Wiesbaden, Germany) were used. The cells were loaded in the dark with the Ca^{2+} indicator Fura 2-AM (#11524766; Molecular Probes) dissolved in DMEM/HG serum-free medium (ADD651C; Sigma) enriched with 1% BSA (bovine serum albumin) and incubated for 60 min at 37°C. After washing the cultures in DMEM/HG with 10% FCS, cultivation of the cells continued up to 60 min at 37°C.

After the incubation time specified in the figures, the neurons were stimulated with 200 μM L-glutamate and 50 μM glycine in Ca^{2+}-containing Locke's solution [154 mM NaCl, 5.6 mM KCl, 3.6 mM $NaHCO_3$, 2.4 mM $CaCl_2$, 5.6 mM glucose, and 10 mM HEPES (4-(2-hydroxyethyl) piperazine-1-ethanesulfonic acid); pH 7.4] and the changes in the level of intracellular Ca^{2+} were determined [83,84]. Before stimulation with glutamate and glycine, the neurons were exposed to the amyloid peptide in the absence or presence of Na-polyP by pre-incubating the cultures with Aβ(25−35) at a final concentration of 10 or 30 μM and 50 μg/mL of Na-polyP (average chain length, ≈40 P_i units) in DMEM/HG serum free medium. In the controls without Aβ(25−35) and Na-polyP, only 200 μM glutamate and 50 μM glycine or 50 μM glycine were added at the start of the Ca^{2+} measurements. The Ca^{2+} level was measured using an Olympus IX70 microscope connected with the UApo40X:340 apochromatic reflected light fluorescence objective, alternately illuminated with light of wavelengths 340 and 380 nm. Registration was performed with a CCD camera, model C2400–77 (Hamamatsu, Herrsching, Germany). Subsequently, the fluorescence ratios 340:380 nm were determined; the emission peak remains at 510 nm [85,86]. Data are presented as means ± SEM; 10 replicate measurements from 3 independent cultures were performed. Statistical significance was determined by one-way ANOVA and Scheffe's test.

2.9. Preparation of the serotonin-Ca^{2+}-polyP-based coacervate

Na-polyP dissolved in distilled water was mixed with an aqueous solution of serotonin hydrochloride. Then a $CaCl_2$ solution (prepared from $CaCl_2 \bullet 2H_2O$) was added and the pH was adjusted to 7.3. Thereafter, the mixture was stirred at room temperature for 3 h to allow coacervate formation. The final concentrations of the components in the mixture were as follows: 47 mM serotonin, 1.18 mM $CaCl_2$, and 39 mM Na-polyP (based on P_i; this corresponds to 4 mg/mL of Na-polyP).

2.10. Preparation of the serotonin-Ca^{2+}-polyP-based nanogels and nanoparticles

The procedure is based on the previously described strategy [57,87]. The liquid-liquid phase separation in an aqueous milieu is driven by a series of noncovalent interactions (mainly by hydrogen bonding, electrostatic interaction, and cationic π interactions) [88].

To prepare the serotonin-Ca^{2+}-polyP-based nanogel, chitosan (degree of deacetylation, 75–85%; #C3646; Sigma-Aldrich) was dissolved at a final concentration of 10 mg/mL in 1% (v/v) acetic acid at 60°C with stirring and then filtered using a 1000 mesh microporous membrane. After adjustment of the pH to 6, a solution of serotonin hydrochloride (final concentration, 100 mg/mL) and $CaCl_2$ (final concentration, 5 mg/mL) in distilled water was added, followed by addition of an aqueous Na-polyP solution (final concentration, 50 mg/mL) and adjustment of the pH to 7. Immediately after addition of the Na-polyP solution, 4-arm-poly(ethylene glycol)-*N*-hydroxysuccinimide (4-arm-PEG-NHS; #A44023–5K from Biopharma, Watertown, MA, USA) was dropwise added at room temperature for 1 h with vigorous stirring until a final concentration of 10 mg/mL was reached. The obtained nanogel formulation was washed in water and stored at 4°C after

lyophilization.

The initial steps for the fabrication of the serotonin-polyP-based nanoparticles were identical to the steps used for the nanogel formulation, except that after addition of the Na-polyP solution the pH was adjusted to 10 with NaOH. Again, immediately thereafter, the 4-arm-PEG-NHS solution was dropwise added at room temperature for 1 h under vigorous stirring until a concentration of 10 mg/mL was reached. To support nanoparticle formation, the pH of the reaction mixture was continuously controlled and kept at pH 10. The nanoparticles were collected by centrifugation and washed in water. After lyophilization the particles were stored at 4°C.

2.11. Preparation of the serotonin-Ca^{2+}-polyP-loaded nanoparticle-micelles

Basically, the technique used was based on the protocol proposed by Kreuter et al [89]. Briefly, a 1% dextran 70000 (Invitrogen; 63303 Dreieich; Germany Dextran, SNARF, 70,000 MW, anionic) solution was prepared in 0.1 N HCl supplemented with 20 mM $CaCl_2$. The negative charges exposed on the polymer are linked to polyP *via* Ca^{2+} bridges. In parallel, a 35 mM serotonin-hydrochloride solution was prepared in distilled water. This solution was added to the acidic, Ca^{2+}-containing dextran solution at a ratio (v/v) of 0.2:1. Then, after mixing, an aqueous solution of 3 mg/mL (35 mM; based on P_i) of Na-polyP was added at a ratio (v/v) of 0.2:1. Immediately thereafter, butyl cyanoacrylate (#181404; Sigma-Aldrich) was added to this mixture to obtain a final 1% nanoparticle suspension. To allow nanoparticle formation, the mixture was stirred for 5 h. After neutralization with 0.1 N NaOH, the solution was filtrated through a bacterial exclusion membrane. Finally, a solution of 1% D-(+)-glucose (anhydrous; # APO456788065; Sigma-Aldrich) was added for final re-dispersion. The solid material was lyophilized and stored at 4°C.

For the preparation of nanoparticle-loaded micelles capable of crossing the blood-brain barrier, the serotonin-polyP-loaded nanoparticles were supplemented with 1% polysorbate after suspension (with sonication) in PBS or simulated nasal fluid (see below) at a Na-polyP concentration of 5 mg/mL.

2.12. Formulation of a nasal spray

In view of a potential medical application, a composition suitable for a nasal spray was developed. The basal pH of the spray was adjusted to 7.4 using a phosphate buffer (NaH_2PO_4/Na_2HPO_4). The coacervate nanogels, nanoparticles and nanoparticle-micelles Na-polyP were included at a final concentration of 15 mg/mL. Propylene glycol (20% v/v final concentration) was added as humectant to keep the epithelia moist and to provide the fluid with antibacterial and antifungal properties [90]. The solution is intended for use in a nasal vaporizer [91]. To determine the release of the active polyP ingredient, phosphate-free simulated nasal fluid was used instead of the NaH_2PO_4/Na_2HPO_4 buffer.

2.13. Release studies with the coacervate or nanoparticles

The release studies were performed in simulated nasal fluid composed of 7.45 g/L NaCl, 1.29 g/L KCl, and 0.32 g/L $CaCl_2 \times 2H_2O$ in distilled water [92]. The quantitative Phosfinity Quant Kit (Aminoverse B.V., HK Nuth, The Netherlands) was used, as described [93]. Samples of the coacervate nanogel formulation, nanoparticles or nanoparticle-micelles, each loaded with 600 μg of polyP, were incubated in 1 mL simulated nasal fluid at 37°C in a 5% CO_2 incubator. An aliquot of 500 μL was taken and assayed with the enzymatic hydrolysis kit running with yeast exopolyphosphatase. In parallel, a standard curve was compiled and used for the quantification. Each value represents data from five independent experiments. The percentage of polyP released is given in the figure and refers to the total amount of polyP present in the assays (600 μg/mL).

2.14. Microscopic analyses

High resolution SEM images were taken with a Zeiss Gemini 1530 (Zeiss Oberkochem; Germany). For low resolution SEM studies, an ESEM XL-30 microscope (Philips, Eindhoven; Netherlands) was used. The samples were freeze-dried prior to inspection.

Transmission electron microscopic (TEM) observations of the micelles were performed with a Tecnai 12 microscope (FEI Electron Optics, Eindhoven; Netherlands) as previously described [94]. The samples were fixed in paraformaldehyde and glutaraldehyde, then embedded in agarose and finally in LR-white resin (#62661; Sigma-Aldrich). Then ultrathin sections (80 nm) were cut (Microsystems, Wetzlar; Germany).

2.15. Statistics

After calculating that the values are distributed along the standard Gaussian normal distribution and that the variances of the respective groups are equal, the results were statistically evaluated using the independent two sample Student's *t*-test [95]. The data are presented as mean ± SD or mean ± SEM. The significance is indicated by $^* p < 0.01$. In the Fura-2 calcium imaging studies, statistical significance was determined by one-way ANOVA and Scheffe's test.

3. Results

3.1. Dependence of Aβ(25−35) toxicity on preincubation

As previously observed, the neurotoxicity of the amyloid β Aβ (25−35) peptide depends on the time the peptide remains in distilled water [46]. In our experiments, we found that the folding process of the Aβ(25−35) monomers into β-sheets [36] takes 2–5 days; in this process, the neurotoxic Aβ(25−35) amyloid, Aβ(25−35)-a, is formed from the inactive amyloid Aβ(25−35)-i. Considering recent data, we explain this transition as a conformational change from an α-helical to a β-sheet structure (reviewed in ref [36]). When added immediately to the neuronal cultures, no signs of cell death were observed; the morphology of the neurons was indistinguishable from the controls (Fig. 2 (I-A and B)). The neurons retained their characteristic morphology along both their axons and their apical dendrites. In contrast, in the cultures incubated with Aβ(25−35)-a, the neuronal projections were loosened (pre-incubation period: 2 d; Fig. 2 (I-C)) and were finally absent in the assays with the amyloid preparation preincubated for 5 d (Fig. 2 (I-D)).

3.2. Characteristic DNA fragmentation during incubation of neurons with amyloid

Upon exposure to Aβ(25−35)-a, neurons undergo apoptosis, which is accompanied by controlled fragmentation of nuclear DNA [17,46]. The data presented here indicate that a pre-incubation period of 3 or 5 d is required for efficient conversion of the inactive neurotoxic Aβ(25−35)-i (Fig. 2 (II; lanes a to c)) into neurotoxic Aβ(25−35)-a (Fig. 2 (II; lanes d and e)). The initial, non-pretreated Aβ(25−35)-i sample does not affect the integrity of the nuclear DNA of neurons during the 3-d post-incubation with the cells (Fig. 2 (II-lanes a to c). In contrast, after pre-treatment of the Aβ(25−35) monomers for 3 or 5 d, the resulting Aβ (25−35)-a sample causes the formation of ≈ 180-bp fragments and multiples thereof (Fig. 2 (II-lanes d and e)).

3.3. Effect of the amyloid β-protein fragments on cell growth/viability of neurons

Incubation of the primary neuronal cells with the neurotoxic Aβ (25−35)-a peptide (obtained after a 5-day pre-incubation period) led to a significant decrease in the number of viable cells (cell survival rate) to 75.3% after only a 24 h incubation period compared to control (time zero), as determined by MTT assay (Fig. 3). After 72 h, the cell survival

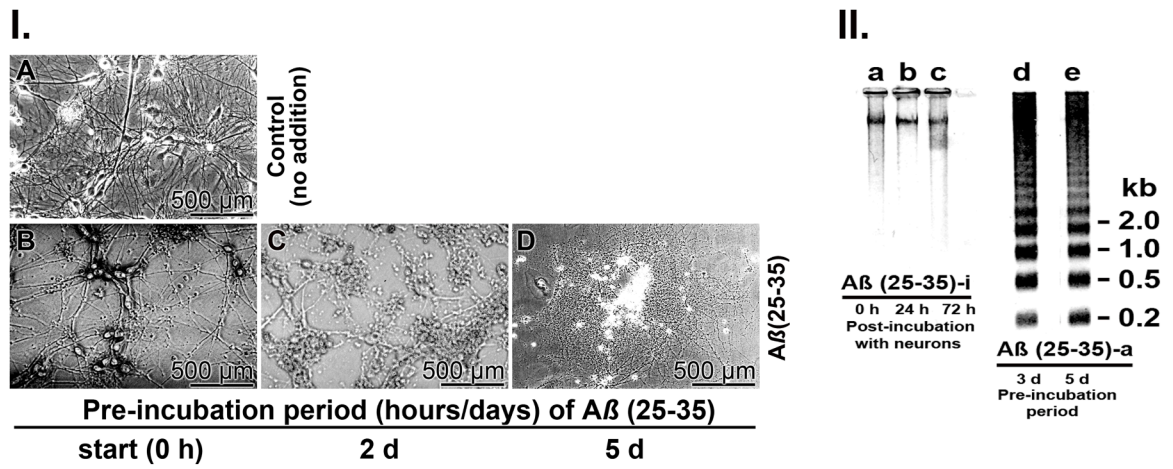

Fig. 2. Effect of β-amyloid (Aβ) on neurons before and after processing from the non-toxic peptide Aβ(25−35)-i to the neurotoxic peptide Aβ(25−35)-a by pre-incubation in distilled water at 4°C for 2–5 days. (I) Immediately after dissolution of the peptide (pre-incubation period, 0 h) (A and B), no notable adverse effects on the morphology of the neurons were observed compared to the control (without peptide addition). (C and D) The processed (Aβ) peptide (Aβ(25−35)-i), converted into the neurotoxic form Aβ(25−35)-a, caused increasing signs of apoptotic cell death (degradation of the neurons) after only 2 days of preincubation, which intensified after the 5-day preincubation period. (II) Neurons treated with Aβ(25−35)-i for 0–72 h (lanes a to c) show no DNA fragmentation pattern, whereas neurons treated with Aβ(25−35)-a activated by pre-incubation for 3 (lane d) or 5 days (lane e) show progressive DNA fragmentation during the 72-h post-incubation period.

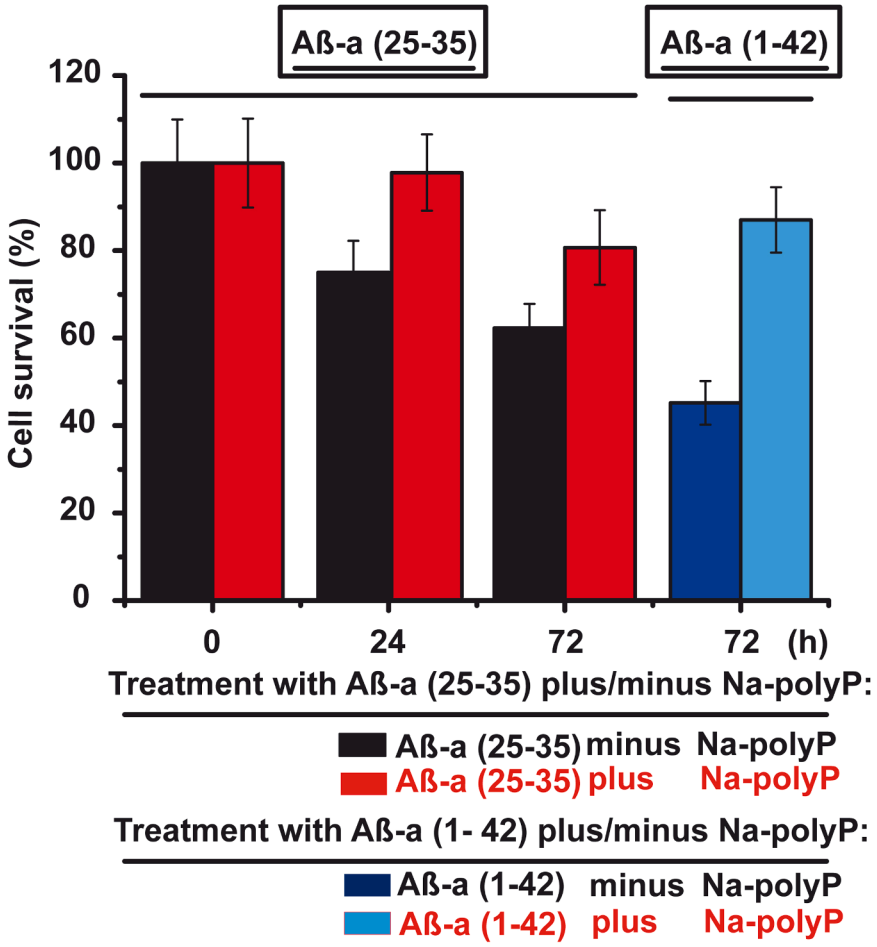

Fig. 3. Protective effect of Na-polyP against the toxic effects of the amyloid β-peptide Aβ (25−35) compared to Aβ (1−42) in primary rat cortical neurons. The cells were incubated for 0–72 h with either the short amyloid β-protein fragment Aβ-a (25−35), or with the longer peptide Aβ-a (1−42), both in the absence or presence of 50 µg/mL of Na-polyP. Equimolar concentrations (10 µM) of the peptides were used. Cell viability was determined by the MTT assay. Cell survival rates were calculated and expressed as % to the start of incubation. The data represent mean ± SD from 6 independent experiments (*$p < 0.05$).

rate further decreased to 62.3%. This decrease in cell viability was significantly reduced when the cells were co-incubated with Na-polyP. The cell survival rates increased to 98.8% (24 h) and 81.2% (72 h), respectively. This mitigating effect of Na-polyP on amyloid neurotoxicity was also observed with the longer peptide Aβ(1−42)-a fragment; the cell survival rate increased from 45.9% to 88.2% (72 h) (Fig. 3).

3.4. Coacervate formation of polyP in cerebrospinal fluid

In addition to cellular components, the cerebrospinal fluid contains marker cells for Alzheimer's disease [96], the $CD8^+$ T effector memory cells. Furthermore, the ionic composition and pH of the cerebrospinal fluid determine the stability and functional effects of drugs [97]. In particular, the Ca^{2+} concentration is a functionally crucial component of the cerebrospinal fluid [61].

The neurotransmitter serotonin was added to promote the coacervation process of the polyanionic polyP. This compound is known to form cationic oligomers [77]. The chosen Ca^{2+} level in the artificial cerebrospinal fluid was 1.18 mM $CaCl_2$ [61]. Upon addition of just 39 mM polyP (4 mg/mL of Na-polyP) to the fluid containing 47 mM serotonin and 1.18 mM $CaCl_2$, an opalescent precipitate formed (Fig. 4 (I-A)). In the absence of serotonin after a short period of 5 min, deposits with a granular surface developed (Fig. 4 (I-B)); the size of the nanoparticles measured ≈ 10 nM. A longer incubation of 4 h resulted in a smoother surface after drying the sample and subsequent SEM inspection (Fig. 4 (I-C)). The addition of 47 mM serotonin to the

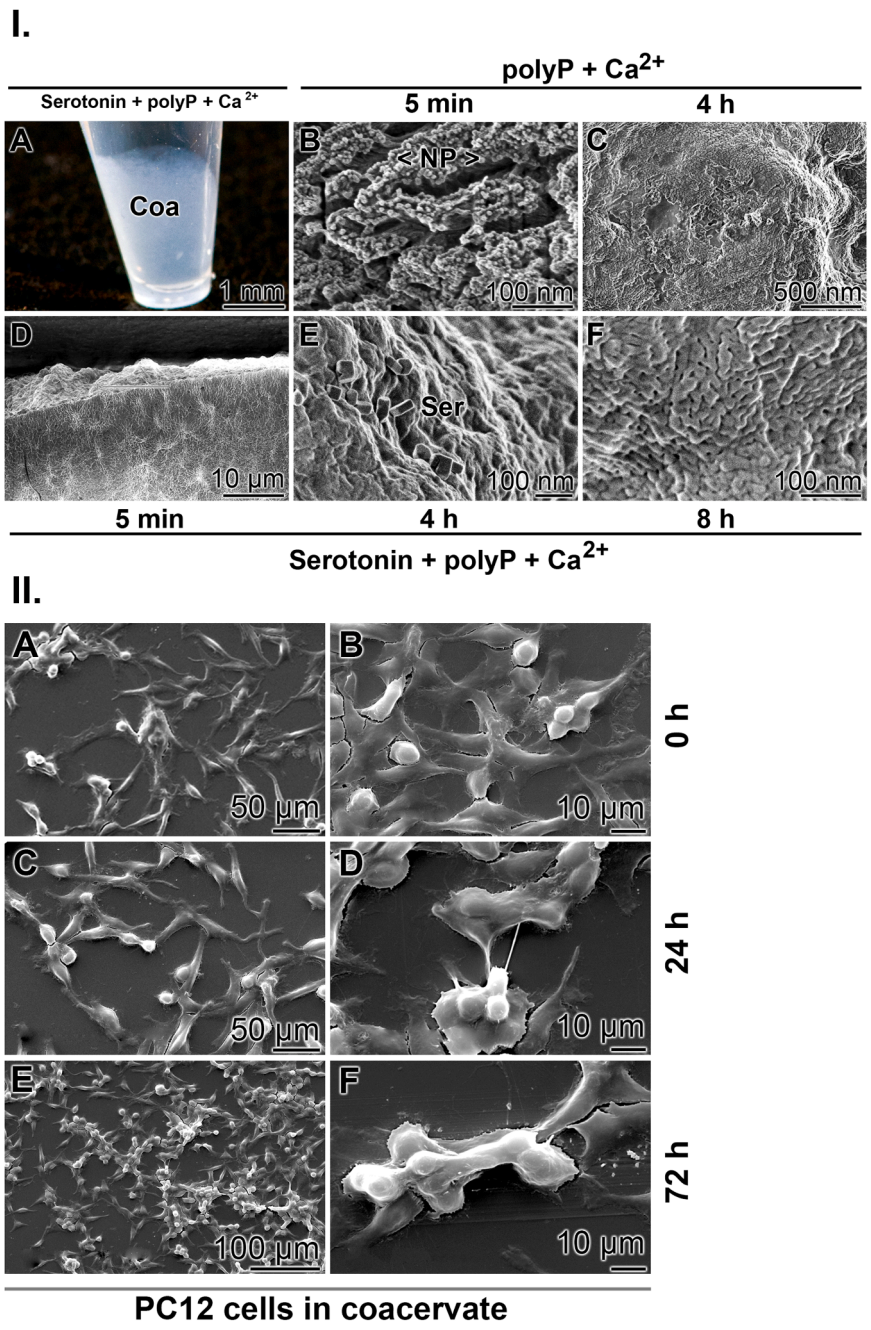

Fig. 4. Preparation of the polyP coacervate with added serotonin. (I) (A) The polyP coacervate (Coa) was formed with serotonin together with Ca^{2+}. (B) After a short incubation time (5 min), the deposits formed in the absence of serotonin showed some granular nanoparticles (NP). (C) Later (4 h), gelatinous coacervate layers formed. (D to F) The coacervate formed in the presence of Ca^{2+} plus serotonin persisted throughout the 8-h incubation period. (II) Neuronal-PC12 cells were overlaid with a coacervate layer formed by Ca^{2+}, serotonin, and Na-polyP and inspected immediately after culturing (A and B) or (C and D) after 24 h and (E and F) after 72 h.

polyP-supplemented reaction mixture changed the morphology in the SEM examination. A compact coacervate was formed after only 5 min and remained throughout the 8 h incubation period (Fig. 4 (I-D to -F)).

To investigate whether the neuronal-PC12 cells are affected by contact beneath the coacervate layer, the cells were covered with 100 μL of the Ca^{2+}, serotonin, and Na-polyP solution per 1 mL medium/serum. The coacervate layer formed immediately (Fig. 4 (II-A and B)) and remained stable for 24 h and 72 h (Fig. 4 (II-C to -F)). Furthermore, cell proliferation was monitored during the final period up to 72 h (Fig. 4 (II-E and -F)). The images showed that the cell number increased strongly during the 24 h to 72 h incubation period. This effect, an obvious decrease at 24 h and a subsequent increase at 72 h, could be attributed to initial stress exerted by the coacervate layer formed during the short 24-h incubation period. Cell viability/growth measured after 72 h did not differ significantly from that of PC12 cells measured in the absence of the polymer, as demonstrated by the MTT assay (decrease in cell viability/growth to 76% after 24 h, but increase to 106% after 72 h). This is consistent with previously published results [63].

3.5. PolyP prevents apoptosis of neurons

The blood platelets play a central role in brain function [98]. They are essential not only for maintaining immune defense, for example, through their involvement in various signaling processes in both innate

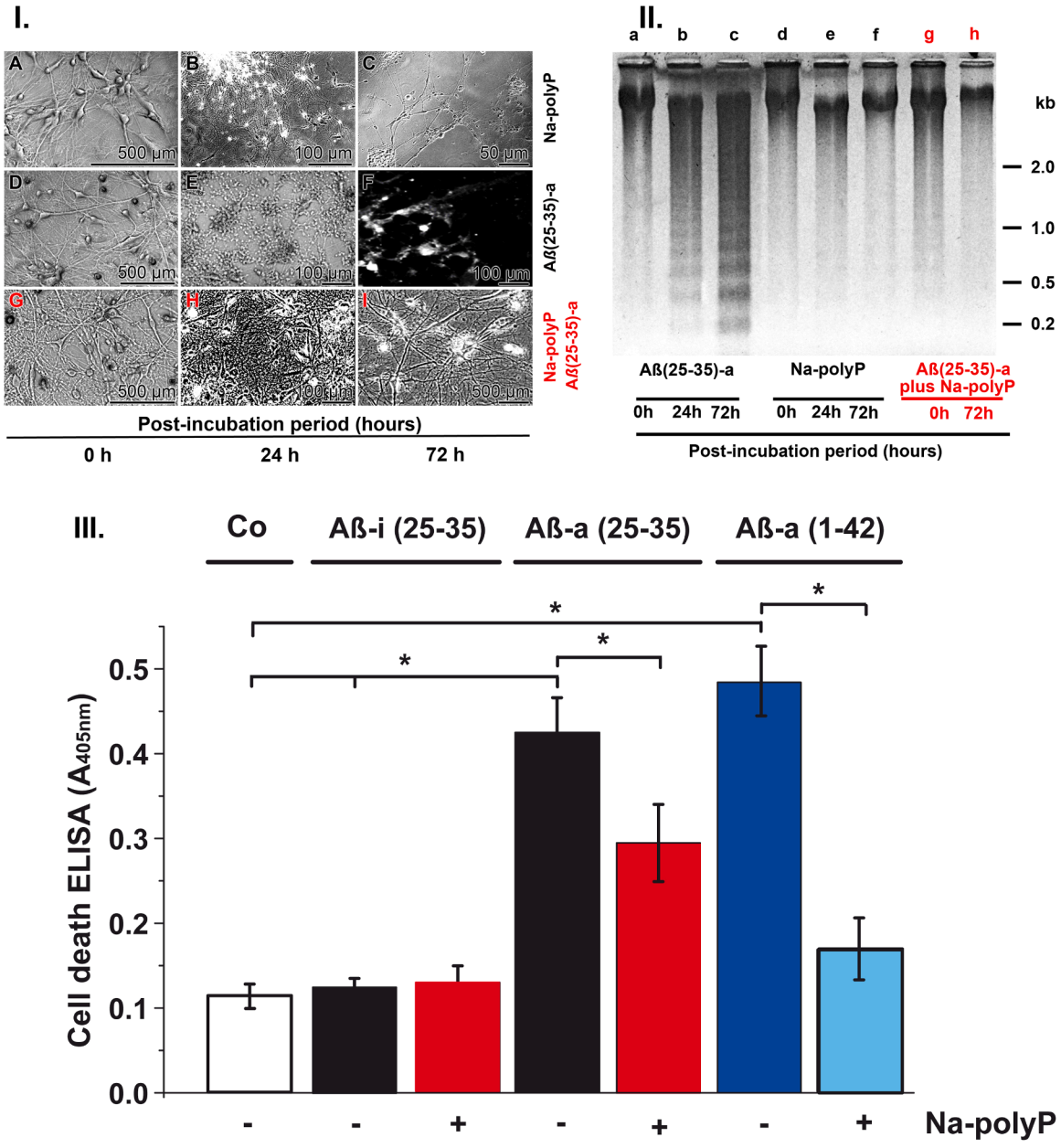

Fig. 5. Prevention of apoptosis in the presence of polyP. (I) (A to C) Incubation of neurons in the presence of 50 μg/mL Na-polyP; no β-amyloid was added. (D to F) Complete apoptotic death after exposure of neurons to Aβ(25−35)-a. (G to I) Prevention of apoptosis after co-incubation with Aβ(25−35)-a and Na-polyP. (II) Fragmentation of nuclear DNA (lanes a to c) after incubation of the cells for 0 h, 24 h, and 72 h with Aβ(25−35)-a. (Lanes d to f) After exposure of the neurons to Na-polyP, no fragmentation occurs. (Lanes g and h) When neurons are co-incubated with Aβ(25−35)-a and Na-polyP, the nuclear DNA also remains intact. (III) Quantification of cytoplasmic histone-associated DNA fragments occurring after treatment of the cultures for 72 h with an equimolar concentration (10 μM) of either the non-toxic peptide Aβ(25−35)-i or the neurotoxic peptide Aβ(25−35)-a, in the absence or presence of 50 μg/mL of Na-polyP, compared to untreated control (Co; without peptide and Na-polyP). In addition to the short Aβ(25−35) peptide fragments, the neurons were also exposed to the longer Aβ(1−42)-a peptide (10 μM). Apoptosis was determined using photometric cell death detection ELISA. The means ± SD of 6 independent experiments are shown. *$p < 0.01$.

and adaptive immune responses [99], but also for the physiological functionality of neurons. Both systems – immune function and interaction within the neuronal network – are already linked during the processing of megakaryocytes into platelets [100]. The 200 – 300 nm sized dense granules in the platelets are filled with polyP as well as ADP, ATP, Ca^{2+}, and neurotransmitters, especially serotonin. These components are released upon activation of the platelets by ADP, thrombin, or collagen. Systemic inflammation, neurovascular dysfunction, and coagulopathy are equally common in neurological pathologies such as Alzheimer's and Parkinson's disease or multiple sclerosis [101].

Experimental data suggest that the release of serotonin from platelets occurs *via* co-transport with polyP, a view supported by the fact that the two molecules can form salt-like deposits at physiological pH [102]. There is also evidence that these two molecules are functionally linked with regard to the neurotoxicity caused by Aβ(25−35)-a. Therefore, we co-incubated the neuronal culture with 50 μg/mL of Na-polyP, a higher concentration than the 7.81 μg/g present in 12-months-old rats [103], but lower than the amount of polyP required for the activation of skin keratinocytes [51]. This higher concentration should also compensate for the age-related down-regulation of the polyP levels in the brain [103].

The neuronal cultures exposed to 50 μg/mL of Na-polyP did not alter the morphology and network of axons during the chosen 72 h incubation (Fig. 5 (I-A to -C)). In contrast, supplementation of the cultures with 10 μM Aβ(25−35)-a resulted in a strong and almost complete removal of the cells (Fig. 5 (I-D to -F)). After co-incubation of the neurons with 50 μg/mL of Na-polyP together with 10 μM Aβ(25−35)-a, complete protection from cell death was observed (Fig. 5 (I-G to -I).

To verify that the cell death was due to programmed cell death, the DNA fragmentation assay was chosen [80]. This series of experiments confirmed the cell biological findings (Fig. 5 (II)). The cells exposed to Aβ(25−35)-a showed progressive DNA fragmentation with a maximum after 72 h (Fig. 5 (II lanes a to c)). Cells incubated with 50 μg/mL of Na-polyP showed no signs of nuclear DNA fragmentation (Fig. 5 (II lanes d to f)). The same applied to the analyses of nuclear DNA integrity in the co-incubation studies with 10 μM Aβ(25−35)-a and 50 μg/mL of Na-polyP (Fig. 5 (II lanes g and h)), even during the 72-h incubation period.

For quantification of apoptosis, a photometric enzyme immunoassay (cell death detection ELISA) that measures apoptosis by quantifying cytoplasmic histone-associated DNA fragments was used. As shown in Fig. 5 (III), treatment of the cells for 72 h with 10 μM Aβ(25−35)-a lead to a significant, 3.7-fold increase in cell death ($A_{405\ nm}$ value) compared to control (absence of any additives), while incubation of the cells with the same concentration of the non-toxic peptide Aβ(25−35)-i has no significant effect. Addition of 50 μg/mL of Na-polyP markedly reduced the increase in the rate of apoptosis (by 41%). For comparison, the induction of apoptosis by the likewise neurotoxic Aβ(1−42)-a (used at an equimolar concentration) was determined. The results revealed an even but not significantly higher increase in $A_{405\ nm}$ value compared to the shorter Aβ(25−35)-a peptide (321% increase in cell death rate compared to control). Again, the rate of apoptosis strongly and significantly decrease when the cultures were co-incubated with Na-polyP.

3.6. PolyP inhibits Ca^{2+} influx in neurons

To confirm these data, an independent series of experiments was conducted in which the intracellular Ca^{2+} level was measured in dependence on contact with the neurotoxic β-amyloid Aβ(25−35)-a in the absence or presence of Na-polyP [8,104]. The rise of Ca^{2+} concentration due to the influx of Ca^{2+} *via* the NMDA receptor [23] is induced by addition of the receptor agonist glutamate and glycine [8].

In the Ca^{2+} influx studies summarized here, the neurons were preincubated for 30 min with 10 μM or 30 μM Aβ(25−35)-a, with or without 50 μg/mL (490 μM in terms of P_i units) of Na-polyP. The intracellular Ca^{2+} levels were measured using the esterified, cell-permeant Fura 2-AM, which binds to Ca^{2+} and, after cleavage by intracellular esterases, remains trapped within the cells. The data showed that after the addition of 200 μM glutamate and 50 μM glycine to neurons preincubated with 10 or 30 μM Aβ(25−35)-a, a strong, dose-dependent influx of Ca^{2+} occurs within seconds to minutes (Fig. 6-A). The increase in intracellular Ca^{2+} level was significantly lower when the neurons were preincubated with Aβ(25−35)-a in the presence of Na-polyP. Fig. 6-A shows the kinetics of Ca^{2+} influx after preincubation of the cells with 30 μM Aβ(25−35)-a and 50 μg/mL of Na-polyP. The measured Ca^{2+} levels differ significantly from the values after exposure of the cells to 10 μM and 30 μM Aβ(25−35)-a in the absence of Na-polyP, as indicated in the figure. The changes in Ca^{2+} levels monitored in the experiments with Aβ(25−35)-a plus Na-polyP (Fig. 6-A) were close to the changes measured in controls (Control-I) after stimulation of the neurons with glutamate and glycine without prior exposure of the cells to the Aβ(25−35)-a peptide and Na-polyP (Fig. 6-B). The addition of 50 μM glycine alone (without glutamate) had, if at all, only a very small, statistically not significant effect on Ca^{2+} levels (Control-II). It should be emphasized that the staining of the neurons with Fura 2-AM using the methods applied here does not allow a fine analysis of the intracellular Ca^{2+} levels; in general, the green-stained cells after exposure to Aβ (25−35)-a are homogeneously stained and there is no clear localization of the Fura 2-AM (Fig. 6-C (B)). In the brightfield images, all cells showed a normal morphology; at a wavelength (λ) of 240 nm, only a few cells flashed green, indicating the Ca^{2+} burst is paralleled by apoptotic cell death of the neurons. In addition, some dead and necrotic cells are also highlighted in brown (Fig. 6-C (A and B)).

These data indicate that polyP prevents the enhancement of the glutamate-triggered rise in intracellular Ca^{2+} caused by exposure of the neurons to the active amyloid Aβ(25−35)-a.

3.7. Scavenging excess Ca^{2+} ions by the polyP coacervate in cerebrospinal fluid

To demonstrate that the polyP coacervate formed with polyP in artificial cerebrospinal fluid containing 47 mM serotonin and 1.18 mM $CaCl_2$ (see above) is still capable of scavenging excess Ca^{2+} during Ca^{2+} bursts, 0.4 mL of a Na-polyP solution (0.5 M; based on P_i residues) was injected into a tissue culture dish filled with 4.6 mL of this fluid until a final concentration of 39 mM polyP (4 mg/mL of Na-polyP) was reached; this resulted in the formation of a polyP coacervate (Fig. 7A; see also above). After 30 min, an equal volume of a $CaCl_2$ solution (10 mM) was added (Fig. 7B). Immediately after this, and after an incubation period of 1 h (Fig. 7C), the Ca^{2+} concentration in the fluid outside the coacervate was determined using a quantitative colorimetric calcium assay kit (MAK477; Sigma-Aldrich). The results showed that the Ca^{2+} concentration in the fluid outside the coacervate decreased from 5.2 ± 0.2 mM to 3.9 ± 0.3 mM (n = 6) during this time, indicating that the coacervate can still bind excess Ca^{2+} ions.

3.8. Proposed vehicles for in vivo applications

Unfortunately, almost all potential neuropharmaceuticals cannot penetrate the intact blood-brain barrier [105]. On the other hand, macrophage precursor cells, which emerge from the yolk sac, are among the first immune cells to settle in the brain [106]. Future research will need to clarify whether these cells also transport particulate polyP in their exosomes.

However, several alternative routes exist that could potentially allow polyP to cross the blood-brain barrier. As summarized in the comprehensive review by Wu et al. [105], these include passive transcytosis and the possibility of intranasal administration. The latter option can be implemented in the form of a polyP-containing spray for application to the respiratory tract. We have already developed a spray for such an application, intended to prevent infection of endothelial cells with the coronavirus (COVID-19) [107]. In recent years, we have optimized the

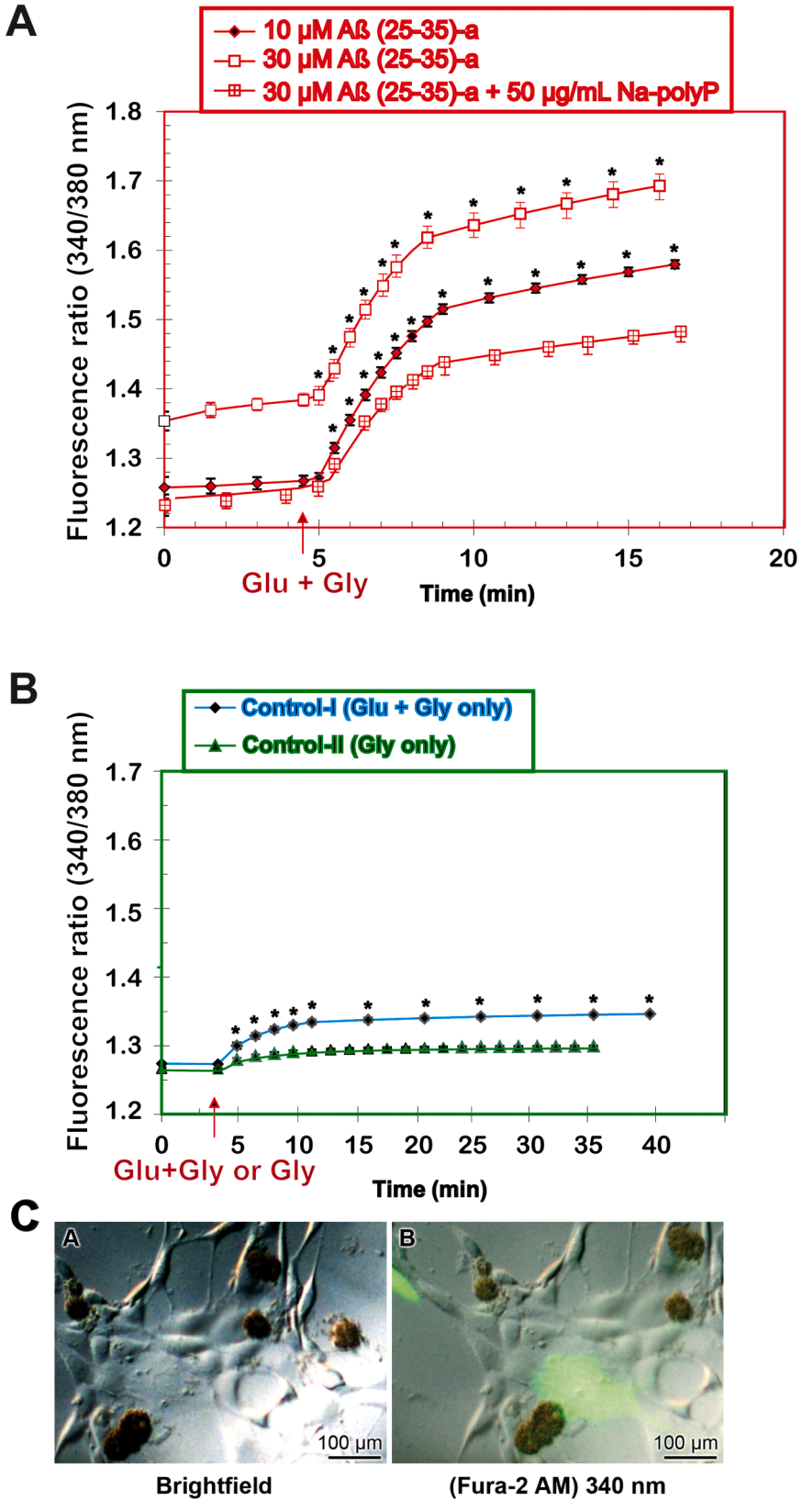

(caption on next page)

Fig. 6. Changes in intracellular Ca^{2+} levels measured with the Fura 2-AM indicator reagent. (A) Pretreatment of the neurons with the Aβ(25−35)-a peptide resulted in a drastic increase in the glutamate-triggered influx of Ca^{2+} ions into the neurons. The Ca^{2+} influx was strongly reduced when the neurons were preincubated with Aβ(25−35)-a together with 50 μg/mL of Na-polyP. Two concentrations of Aβ(25−35)-a (10 μM and 30 μM) were tested for significance levels compared to the rate after coincubation with Na-polyP and marked accordingly (*). The arrow marks the point in time when glutamate and glycine were added. (B) In the controls, the influx rates were measured after stimulation of the cells with 200 μM glutamate and 50 μM glycine (Control-I) or 50 μM glycine alone (Control-II) without pretreatment with Aβ(25−35)-a and Na-polyP. In the presence of glycine alone, the extent of Ca^{2+} influx is only marginal, but is strongly stimulated in combination with glutamate. However, the values for the glutamate-induced influx without prior exposure to Aβ(25−35)-a are still significantly lower than after pretreatment with the peptide, but are close to the values obtained with Aβ(25−35)-a and Na-polyP. (C-A) Brightfield image of neurons preincubated with the neurotoxic Aβ(25−35)-a for 30 min. (C-B) The green flashing areas indicate cells with Ca^{2+} overload that are undergoing apoptosis. However, no distinct concentration differences are measurable within the apoptotic cells (apo). Some dead cells are scattered within the cell layer and appear brown. Data in A and B are presented as mean ± SEM of 10 replicates (10 coverslips) from 3 independent cultures (*$p < 0.01$; Aβ(25−35)-a treated neurons compared with Aβ(25−35)-a treated neurons with Na-polyP, and with control-I). Statistical significance was determined by one-way ANOVA and Scheffe's test.

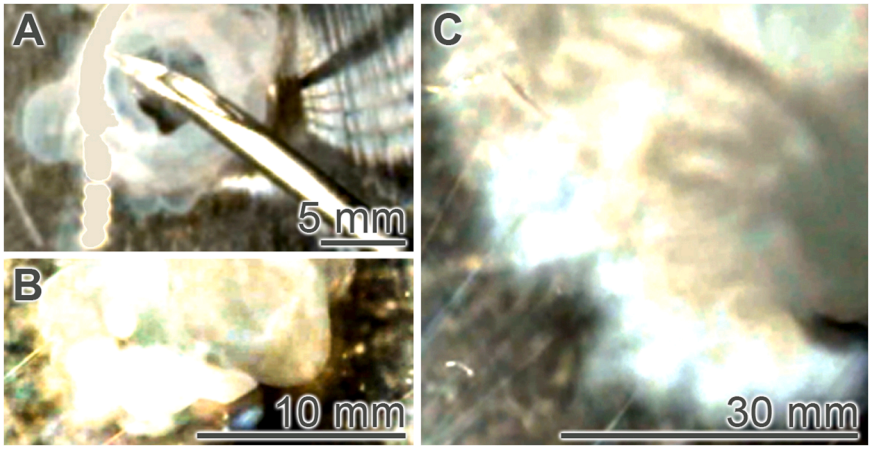

Fig. 7. Morphology of polyP coacervate after injection of a polyP solution into artificial cerebrospinal fluid and subsequent addition of excess calcium ions. (A) Coacervate formation during injection of the Na-polyP solution into a tissue culture dish containing artificial cerebrospinal fluid. (B) The coacervate immediately thereafter and (C) 1 h after addition of a solution with excess Ca^{2+} ions.

formulation to make the spray more biocompatible and to ensure a stable pH of 7.2. The spray contains 15 mg/mL of Na-polyP, a non-cytotoxic concentration.

Here, two further possible dosage forms of polyP, which were fabricated in the present study, are proposed; application of polyP in the form of a polymeric nanogel and as nanoparticles [105,108]. Both formulations are based on the characteristic property of polyP to form a coacervate [57]. Since the Ca^{2+} concentration in the cerebrospinal fluid is low, and inspired by the fact that physiologically polyP and serotonin are colocalized in the dense grana of the platelets, the cationic fraction required for phase separation of the polyanionic polyP was enriched with serotonin, which is positively charged at physiological pH. The

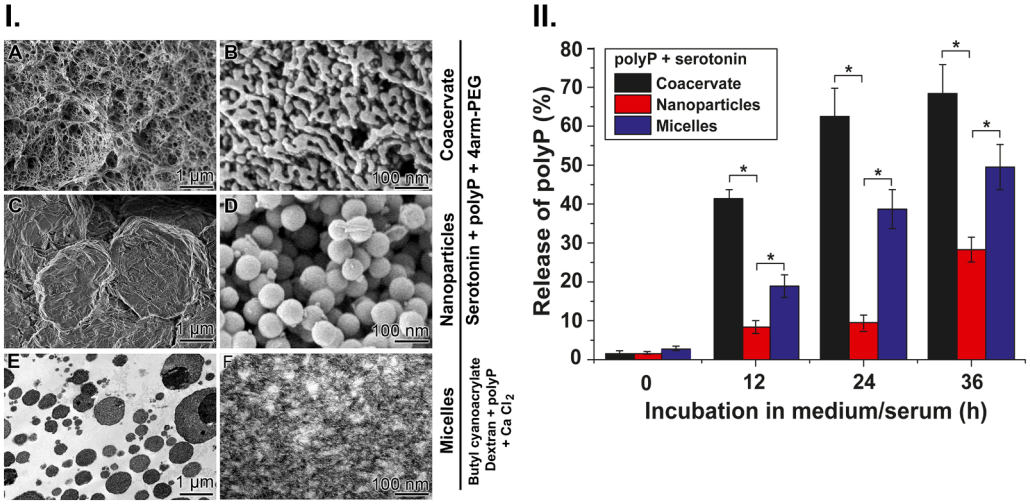

Fig. 8. Three formulations were introduced to target polyP to the brain. (I) The formulations: (A and B) Stable polyP coacervate nanogel prepared with chitosan and a 4-arm-PEG component. (C and D) PolyP nanoparticles prepared in a similar way but at alkaline pH. (E and F) PolyP-containing nanoparticle-micelles prepared with butyl cyanoacrylate and Ca^{2+}. (II) Release kinetics of polyP from the encapsulated depot material. PolyP release was determined in simulated nasal fluid using the quantitative enzymatic hydrolysis technique. The highest release of polyP was measured from the coacervate phase (nanogel), while the nanoparticle form released lower amounts. An intermediate release of polyP was observed from the nanoparticle-micelles prepared with butyl cyanoacrylate and Ca^{2+}. Data represent mean ± SD from 5 independent experiments (*$p < 0.01$).

morphology of the coacervate phase is known to change from spherical to "wormlike micelles" [109]. Exactly, this appearance is observed when a polyP coacervate is prepared with Ca^{2+} together with serotonin (Fig. 8 (I-A and B)). The stability of the polymeric coacervate nanogel was increased by the addition of chitosan and a 4-arm-PEG component, as described in the Materials and Methods section.

The same composition as for the coacervate nanogel formulation (Ca^{2+}, serotonin, Na-polyP together with chitosan and a 4-arm-PEG component) was used to prepare the nanoparticles. The formulation was brought to the desired nanoparticles by adjustment of the pH to 10 before addition of the 4-arm-PEG component. The particle size of approximately 70 nm (Fig. 8 (I-C and D)) corresponds to the size published for other neuropharmacological applications [110].

The third formulation for the spray, capable of crossing the blood-brain barrier [89], is based on an established dextran/butyl cyanoacrylate fabrication process that got a premarket FDA-approval for tissue adhesives for the embolization of arteriovenous brain malformations [111]. The globular samples, with a size of ≈ 600 nm (Fig. 8 (I-E)), exhibit linearly arranged structures that we interpret as Ca-polyP chains (Fig. 8 (I-F)). The main ingredients of the intended nasal nose vaporizer are Na-polyP and propylene glycol, as listed under Materials and Methods.

3.9. *Release studies of the encapsulated polyP: Coacervate – nanoparticles – nanoparticle-micelles*

A newly developed polyP quantification assay based on enzymatic hydrolysis of the polymer was used, which has proven to be a specific method for determining polyP in bioorganic materials [93]. PolyP encapsulated in the three application forms exhibited different release kinetics (Fig. 8 (II)). The fastest release was measured for the coacervate nanogel formulation, where 38% of the available polymer was released from the initial 600 μg/mL of Na-polyP during the first 12 h of incubation in RPMI 1640 medium containing 10% horse serum and 5% fetal bovine serum. The extent increased to 63% (after 24 h) and 72% (36 h). The release from the 4-arm-PEG-based nanoparticles was retarded, reaching 7% (12 h), 9% (24 h), and finally 28% (36 h). The controlled release from the nanoparticle-micelles was also efficient, reaching values of 21% (12 h), 42% (24 h), and 51% (36 h).

4. Discussion

The concentration of polyP in tissues changes with age [27]. The metabolic consequences are far-reaching. They are associated, in particular, with a deterioration in the energy balance [112] and Ca^{2+} homeostasis, including an impaired control of the formation of reactive oxygen species (ROS) [113]. Furthermore, the reduction in mitochondrial polyP levels affects the function of this organelle and accelerates the senescent phenotype [112,114]. This can be measured when polyP is depleted upon oligomycin poisoning of ATP synthase. In addition, polyP controls platelet activation, including APP expression and serotonin release [115].

ATP acts not only intracellularly but also extracellularly as a neurotransmitter in the central nervous system *via* the purinergic signaling circuit [116]. In tissues and cell assemblies, ATP is generated enzymatically from polyP *via* ALP and ADK [53] after it is converted into the coacervate phase. This conversion is achieved by adding Ca^{2+} to polyP [58]. In the present study, neurons were exposed to the Aβ (25−35)-a peptide, which is toxic not only to neurons [117] but also to PC12 cells [118]. The underlying mechanism is based on impaired mitochondrial bioenergetics and sensitization of the NMDA receptor [119]. This leads to an enhanced influx of Ca^{2+} triggered by glutamate, followed by neuronal apoptosis, an effect that can be mitigated by memantine [17] and flupirtine [117,120]. The active anti-amyloid ingredient is polyP, which is delivered to the NMDA receptor both from within the cell (from the mitochondria) and extracellularly (from the platelets) and acts as a Ca^{2+} chelating agent at the receptor. PolyP is a natural Ca^{2+}-chelating polymer that naturally occurs in the synaptic regions [121] and thus can avoid the use of cell-permeable synthetic chelators [122].

For comparison, the longer peptide Aβ(1−42), which is also neurotoxic to primary neuronal cell cultures, was used in some experiments. The toxicity of this amyloid peptide fragment was also significantly reduced in the presence of Na-polyP. However, the underlying mechanism may differ from that of the shorter peptide Aβ(25−35), which lacks the glutamate residues Glu11 and Glu22 present in Aβ(1−42) that are involved in the nucleation and salt bridge formation of the amyloid fibril [123].

PolyP has been implicated in a number of neurodegenerative diseases such as amyotrophic lateral sclerosis, frontotemporal dementia, as well as Alzheimer's and Parkinson's disease [124]. The underlying mechanisms have been proposed to include a reduction/impairment of the mitochondrial activity [125], dysregulation of mitochondrial Ca^{2+} homeostasis [126], neuronal apoptosis and protection [25], intracellular cell signaling [127], and neuro- and glio-transmission [128]. The basic metabolite for the intracellular synthesis of polyP in eukaryotic systems is ATP, which is synthesized in mitochondria (reviewed in: refs [53,129]). PolyP is released particularly from platelets upon activation [55,56]. In addition, activated mast cells, which share many structural and functional properties in common with macrophages, distribute and release the polymer [130]. With regard to neurodegenerative diseases, it is important to note that the polyP content in the brain changes significantly during aging [103]. The content in embryos (18 days) is 38 μM (about 3.04 μg/g tissue); in newborn animals 19 μM (5 d old; ≈1.52 μg/g), in young rats (3 months) 110 μM (8.80 μg/g), in middle-age rats (12 months) 122 μM (9.76 μg/g), and in old animals (28 months) only 55 μM (4.40 μg/g) [103]. In an older study [131], it was confirmed that in brain, e.g., from mice, the polyP content is higher at 96 μM than in kidney (64 μM) or liver (38 μM). Furthermore, the concentration also differs in the various cell organelles; in rat brain, the highest levels are found in the nuclei at 160 μM [103]. Platelets contain ≈ 0.74 nmol polyP (59.2 ng) per 10^8 platelets [132] or 67 μg/g (assuming a platelet volume of approximately 8.9 fL) [133].

The Ca^{2+} level in platelets is sufficiently high to enable coacervation of polyP [134,135]. However, outside these cells, e.g. in the cerebrospinal fluid, the pool of free Ca^{2+} may be insufficient to initiate the coacervation process [136]. Therefore, in the *in vitro* studies presented here, the mixture used to study the effect of the polyP coacervate on neuronal cells was supplemented with serotonin, a cation at physiological pH that, despite its positive charge, can cross the cell membrane [137].

For delivery to the target sites in brain tissue, we developed – in a biomimetic approach – vehicles that mimic the conditions under which polyP is present in the dense granules of the platelets. There, polyP is stored at a concentration of 130 mM (in terms of P_i units) [54] together with serotonin and Ca^{2+} ions. Serotonin (pK_a 10.4) [138] is expected to be predominantly in the protonated form at the pH value in the lumen of the dense granules [between pH 5.4 [139] and 6.1 [140,141]]. It is conceivable that, despite the high Ca^{2+} concentration in these cell organelles (2.2 M) [142], the positively charged, protonated serotonin molecules (serotonin concentration in the dense granules: 65 mM) [135] are at least partially bound to the polyanionic polyP. This assumption is supported by the fact that protonated serotonin can associate to form cationic oligomers, facilitated by stacking interactions between the aromatic rings of the monomers [77]. This would allow serotonin, together with polyP, to form a complex coacervate (i.e., a coacervate between polyanionic and polycationic polymers) [143]. In contrast, polyP coacervates known to date are predominantly simple coacervates formed between polyP and divalent cations (mostly Ca^{2+}) [58,144]. The assumption that polyP is associated with serotonin in the dense granules is also supported by the fact that the concentration of free Ca^{2+} ions, which compete with serotonin for binding to polyP, is actually lower in

the granules due to the high content of other anions that can chelate this divalent cation, such as ADP (653 mM) [135] and ATP (436 mM) [135]. Indeed, we were able to demonstrate that under the conditions used in this contribution [39 mM polyP (P_i units), 47 mM serotonin, and 1.18 mM Ca^{2+}], polyP can form a coacervate, forming a gelatinous layer. Furthermore, we found that the coacervate formed under these conditions can continue to bind excess Ca^{2+} ions, which can occur, for example, during activation of the NMDA receptor by neurotoxic amyloid-β protein fragments, most likely *via* an exchange of serotonin cations for Ca^{2+}.

The polyP/serotonin-loaded vehicles described here were designed in such a way that they can reach their target site either in the form of a nanogel or as nanoparticles stabilized with a 4-arm-PEG-based macromolecular system, or as polymeric nanoparticle-micelles, which are able to pass the blood-brain barrier [89]. Such nanoparticle-micelles formed by amphiphilic block copolymers have been identified as powerful vehicles [145]. These core-shell structures can cross the blood-brain barrier within minutes [146]. Transport of the particulate units across this barrier most likely occurs through endocytosis [147]. All three vehicles proposed here demonstrated suitable release kinetics, which are required for potential future applications in the prevention of neuronal damage caused by toxic Aβ-protein in Alzheimer's patients.

There are two direct routes for brain delivery that should be highlighted and will be preferred in future applications; the delivery *via* the olfactory and trigeminal nerves. The olfactory bulb/tract is located at the front of the brain above the nasal cavity, ≈ 7 cm from the nostrils, where it senses the smell (Fig. 9). The trigeminal nerve, the fifth cranial nerve, on the other hand, is responsible for facial sensation and motor functions such as chewing. The cribriform plate of the ethmoid bone is located at the base of the frontal lobe of the brain and allows the passage of the olfactory nerves, facilitating odor perception (Fig. 9B). Below, beneath the epithelial linings, is the lamina propria (a type of loose connective tissue). The olfactory glands (Bowman's glands) secrete the watery mucus that covers the surface of the olfactory epithelium. The basal cells (stem-like cells) regenerate the olfactory receptor neurons. Deeper in the barrier are the epithelial cells that house the olfactory receptor neurons. The olfactory sensory neurons travers the brain barrier and are often decorated with cilia (olfactory receptors, which are G-protein-coupled receptors). Finally, the surface of the olfactory epithelial cells is covered with a mucus layer containing enzymes for degrading odorants, antibodies (IgA), and antimicrobial molecules involved in immune defense. In addition to the transport of bioactive compounds along the neural transport system (the most important routes are olfactory and trigeminal nerve transport), as well as through the lymphatic system to the brain and finally through vascular transport across the functional barrier system, there is an intensive interaction between the tissue environment and the brain [69].

These two routes, the olfactory and trigeminal nerve transport, provide a direct connection between the external environment and the brain [148,149]. The posterior region of the nasal cavity is highly

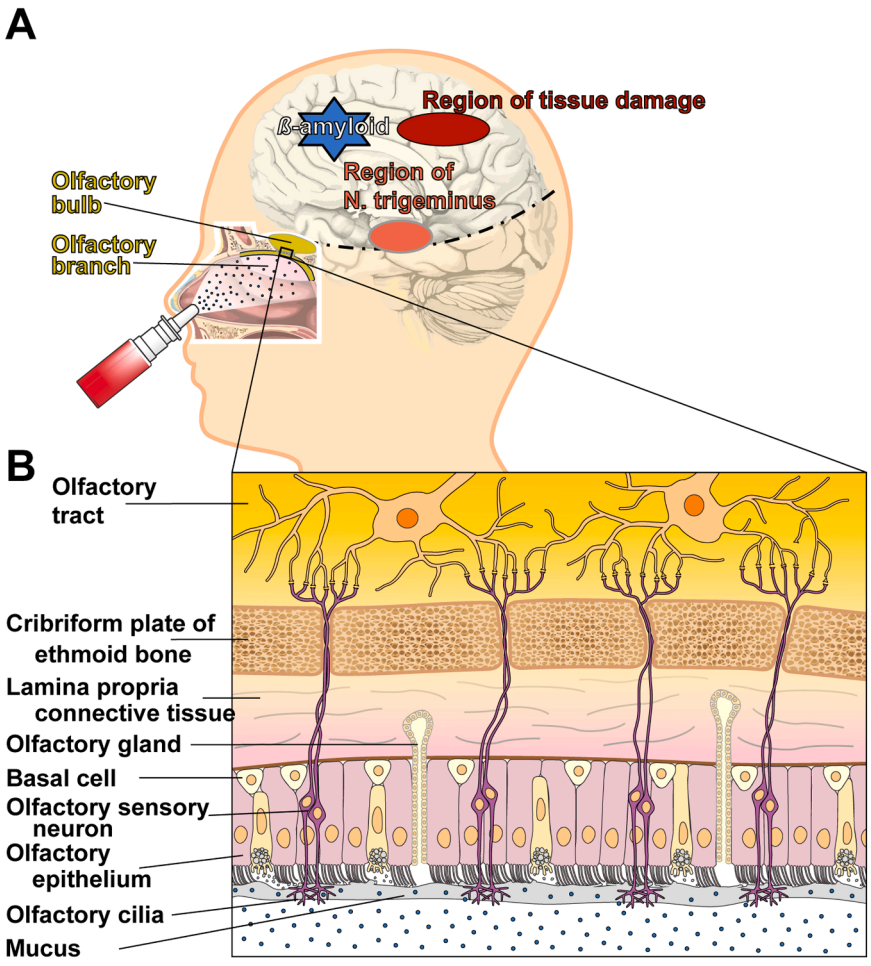

Fig. 9. The olfactory tract provides a direct transport route of administered polyP from the nasopharyngeal cavity to the brain. (A) The main routes of the proposed nasal spray to the neurons with their NMDA receptors are the olfactory and trigeminal nerves. The amyloid Aβ deposits are scattered throughout the brain. The histology of the olfactory tract, which is separated from the blood circulation by the parenchymal and endothelial basal lamina, is complex. The olfactory neurons are layered within the os ethmoidale (ethmoid bone) and the lamina propria (connective tissue) and reach the mucus layer, where the olfactory epithelium is arranged, over which the mucus is secreted.

enriched with olfactory sensory neurons that sense the smell of the inhaled air [150]. Gelling systems/hydrogels [69,151] have been proposed as suitable formulations of a mucoadhesive gel that can overcome the limitations of direct nose-to-brain delivery by prolonging the nasal residence time [152]. They can be administered in the form of orodispersible tablets or as a nasal spray [69]. In our case, for use as a nasal spray suitable for targeted delivery to the brain, the active polymer polyP was formulated in a phosphate buffer (NaH_2PO_4/Na_2HPO_4) solution with a pH of 7.4. Such a formulation would be applied by inserting the spray nozzle into the respective nostril to reach the respiratory mucosa lining the respiratory tract (including the nasal cavity) (Fig. 9-A).

5. Conclusion

Na-polyP is a chelating agent that is found not only in neurons but also in astrocytes [153]. In particular, in mice, polyP levels increase during the development of amyotrophic lateral sclerosis (ALS) and frontotemporal dementia (FTD) and are subsequently released by neurons and astrocytes (Fig. 10–1).

In the present study, the effect of Na-polyP on Aβ(25−35)-induced neurotoxicity was investigated – and a potential solution for application of the significant ameliorating and neuroprotective effect of the physiological polymer is proposed. Based on the published data, it is expected that a Na-polyP-containing nasal spray can be used for the delivery of Na-polyP to the vicinity of the target receptor, the neuronal NMDA receptor, which is inserted into the membranes of the postsynaptic cells of neurons. The reason for the neuroprotective effect of Na-polyP lies in the ability of this polymer to chelate Ca^{2+} (reviewed in refs [57,58,144]).

At the postsynaptic terminals, Ca^{2+} is exported *via* the plasma membrane calcium ATPase pump [154], in conjunction with indirectly acting GABA transporters [155]. The Ca^{2+} influx into the neurons occurs

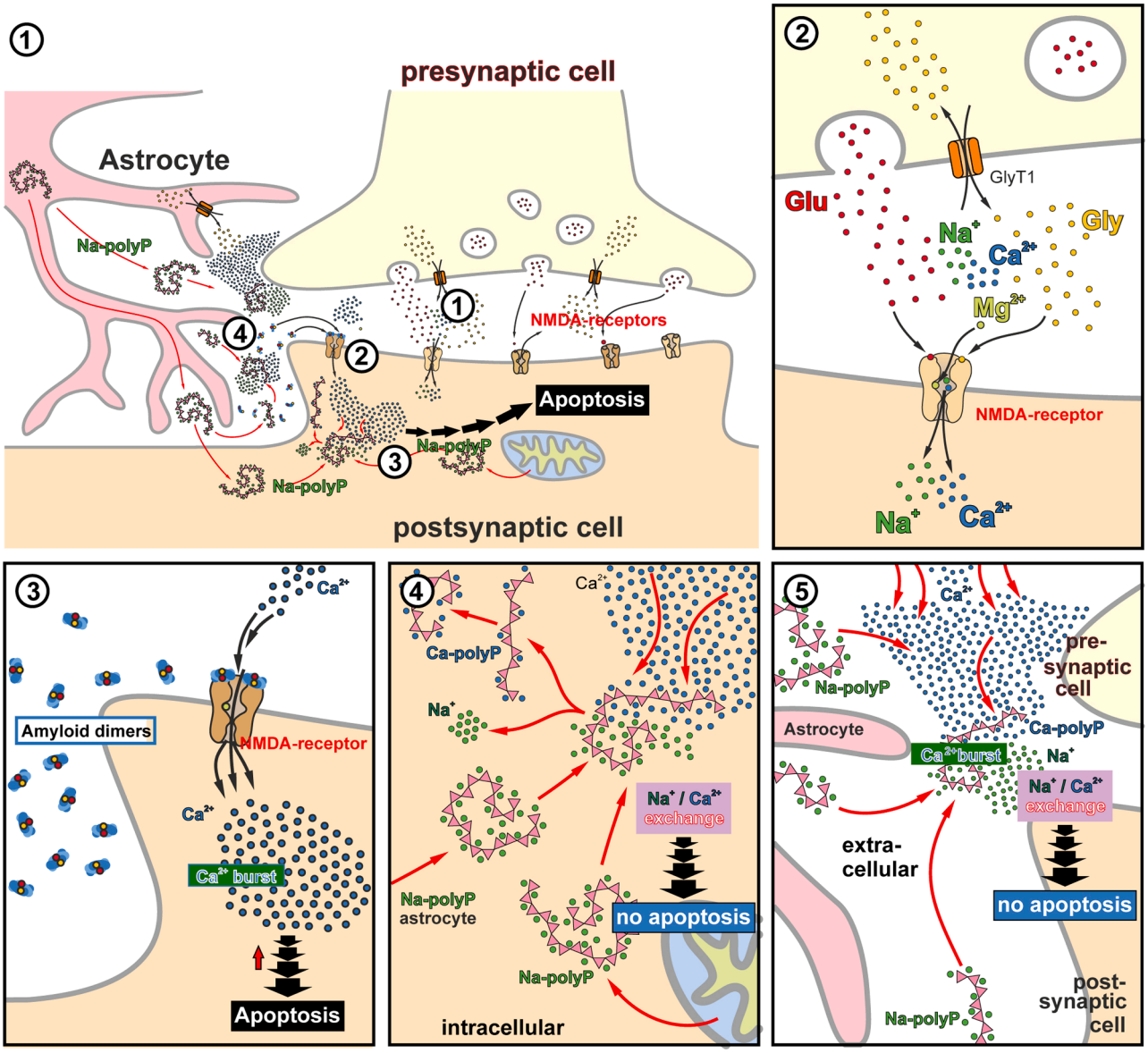

Fig. 10. Sketch of the postulated and partially experimentally supported effect of Na-polyP in neutralizing the neurotoxic, apoptotic effect of Ca^{2+}. (1) Na-polyP is released from astrocytes or neurons and reaches the NMDA receptor, a glutamate (Glu) receptor, which (2) acts as a channel for calcium (Ca^{2+}) and sodium (Na^{+}) ions. (3) In the extraneuronal space, amyloid fragments aggregate into larger units *via* the dimer stage, which sensitizes the NMDA receptor. As a result, the neurons undergo apoptosis. In the presence of Na-polyP, the Ca^{2+} burst in the neurons is attenuated by a Ca^{2+} triggered coacervation process that occurs on both the intraneuronal side (4) and the extraneuronal side of the NMDA receptor (5). The exact intra- and extracellular locations cannot be specified because measurements with the Ca^{2+} indicator Fura 2-AM do not allow for quantification of local differences in Ca^{2+} accumulation.

primarily *via* the NMDA-receptor, which allows the influx of both Na^+ and Ca^{2+} [156]; Fig. 10–2. A cytosolic Ca^{2+} overload can be normalized under physiological conditions by extrusion *via* the PMCA3 Ca^{2+} pump [157]. The Ca^{2+} influx *via* the NMDA receptor leads to an increase in the cytosolic Ca^{2+} concentration [158]; Fig. 10–3. Due to the chelating activity of Na-polyP, an excessive increase in Ca^{2+} levels in the extraneuronal space (Figs. 10–5) and – as measured with the Ca^{2+} indicator Fura 2-AM – most likely also at intraneuronal sites is prevented (Fig. 10–4). Thus, during polyP coacervation, the neurotoxic Ca^{2+} is chelated and thereby removed from the system, particularly from the NMDA receptor, the Ca^{2+}-permeable ligand-gated ion channel involved in excitatory signaling in the nervous system [159]. Na-polyP can therefore be considered a physiological polymer that alleviates amyloid toxicity, as also proposed by Lempart and Jakob [160]. Through this mechanism, *via* coacervation, this polymer prevents further entry of Ca^{2+} into neurons *via* the NMDA receptor and blocks neurotoxicity (Fig. 10–5).

In vivo studies are currently underway using the zebrafish model, which has proven to be an excellent systems for studying neurogenesis [161].

Our next step will the application Na-polyP in a clinical trial in humans. Phase 1 has already been completed, and the data are available to the local ethics committee. We have already prepared the manufacturing process for Na-polyP according to a certified procedure ("Certificate Number RP_01_GMP-2023023_0029) and received the corresponding approval from the European Medicines Agency (EMA). In a recent study (unpublished results [162]), we were able to demonstrate that Na-polyP significantly alleviates the symptoms and supports the healing of neurodermatitis (atopic dermatitis). Interesting, as shown, the platelets also play a central role in this disease.

CRediT authorship contribution statement

Xiaohong Wang: Writing – review & editing, Writing – original draft, Visualization, Validation, Supervision, Resources, Project administration, Methodology, Investigation, Formal analysis, Data curation, Conceptualization. **Schröder Heinz:** Writing – review & editing, Writing – original draft, Validation, Supervision, Project administration, Methodology, Conceptualization. **Hadrian Nassabi:** Writing – review & editing, Writing – original draft, Methodology, Investigation, Formal analysis, Data curation, Conceptualization. **Meik Neufurth:** Writing – review & editing, Writing – original draft, Validation, Methodology, Investigation, Formal analysis, Data curation. **Hiroshi Ushijima:** Writing – review & editing, Writing – original draft, Validation, Supervision, Formal analysis, Data curation, Conceptualization. **Rafael Muñoz-Espí:** Writing – review & editing, Writing – original draft, Methodology, Investigation, Formal analysis, Data curation. **Rita Dobmeyer:** Writing – review & editing, Writing – original draft, Validation, Project administration, Funding acquisition, Formal analysis, Conceptualization. **Sanja Perovic-Ottstadt:** Writing – review & editing, Writing – original draft, Validation, Methodology, Investigation, Formal analysis, Data curation, Conceptualization. **Werner E.G. Müller:** Writing – review & editing, Writing – original draft, Visualization, Validation, Supervision, Resources, Project administration, Methodology, Investigation, Funding acquisition, Formal analysis, Data curation, Conceptualization.

Funding

We acknowledge the financial support of ERC Advanced Investigator Grant (No. 268476) and three ERC-PoC grants (Si-Bone-PoC, Grant No. 324564; MorphoVES-PoC, Grant No. 662486; and ArthroDUR, Grant No. 767234). W.E.G. Müller is holder of the ERC Advanced Investigator Grant and three ERC-PoC grants. The authors also acknowledge the funding from the EU grants CAMAR 8001-CT91–0209 and FAIR5-CT97–3315. Finally, this work was supported by the BiomaTiCS research initiative and the Focus Program Translational Neurosciences (FTN) of the University Medical Center, Mainz.

Declaration of Competing Interest

The authors declare that they have no known competing financial interests or personal relationships that could have appeared to influence the work reported in this paper.

Acknowledgements

The skilled transmission electron microscopy images through the micelles were taken by Dr. Maria Kokkinopoulou (Max Planck Institute for Polymer Research, Mainz; Germany). Her contributions are very much acknowledged.

Data Availability

Data will be made available on request.

References

[1] S. Gehlert, W. Bloch, F. Suhr, Ca^{2+}-dependent regulations and signaling in skeletal muscle: From electro-mechanical coupling to adaptation, Int. J. Mol. Sci. 16 (2015) 1066–1095.
[2] V.G. Vertiprakhov, V.I. Trukhachev, N.A. Sergeenkova, Reflex phase of regulation of pancreatic secretion in poultry after feed intake is associated with gustatory sensations, and neurohumoral-with nutritional value, Front Physiol. 15 (2024) 1341132.
[3] S. Patergnani, A. Danese, E. Bouhamida, et al., Various aspects of calcium signaling in the regulation of apoptosis, autophagy, cell proliferation, and cancer, Int J. Mol. Sci. 21 (2020) 8323.
[4] T.C. Südhof, Calcium control of neurotransmitter release, Cold Spring Harb. Perspect. Biol. 4 (2012) a011353.
[5] R. Yuste, A. Majewska, K. Holthoff, From form to function: calcium compartmentalization in dendritic spines, Nat. Neurosci. 3 (2000) 653–659.
[6] M.P. Mattson, Calcium and neurodegeneration, Aging Cell 6 (2007) 337–350.
[7] J.C. Devedjian, F. Esclapez, C. Denis-Pouxviel, H. Paris, Further characterization of human alpha 2-adrenoceptor subtypes: [^{3}H] RX821002 binding and definition of additional selective drugs, Eur. J. Pharm. 252 (1994) 43–49.
[8] S. Perovic, M. Böhm, E. Meesters, A. Meinhardt, G. Pergande, W.E.G. Müller, Pharmacological intervention in age-associated brain disorders by Flupirtine: Alzheimer's and prion diseases, Mech. Ageing Dev. 101 (1998) 1–19.
[9] K.B. Hansen, F. Yi, R.E. Perszyk, H. Furukawa, L.P. Wollmuth, A.J. Gibb, S. F. Traynelis, Structure, function, and allosteric modulation of NMDA receptors, J. Gen. Physiol. 150 (2018) 1081–1105.
[10] P. Babaei, NMDA and AMPA receptors dysregulation in Alzheimer's disease, Eur. J. Pharm. 908 (2021) 174310.
[11] W. Liu, Y. Li, T. Zhao, M. Gong, X. Wang, Y. Zhang, L. Xu, W. Li, Y. Li, J. Jia, The role of N-methyl-D-aspartate glutamate receptors in Alzheimer's disease: From pathophysiology to therapeutic approaches, Prog. Neurobiol. 231 (2023) 102534.
[12] M. Beaurain, A.S. Salabert, P. Payoux, E. Gras, F. Talmont, NMDA receptors: distribution, role, and insights into neuropsychiatric disorders, Pharmaceuticals 17 (2024) 1265.
[13] M. Lafon-Cazal, S. Pietri, M. Culcasi, J. Bockaert, NMDA-dependent superoxide production and neurotoxicity, Nature 364 (1993) 535–537.
[14] M. Leist, E. Fava, C. Montecucco, P. Nicotera, Peroxynitrite and nitric oxide donors induce neuronal apoptosis by eliciting autocrine excitotoxicity, Eur. J. Neurosci. 9 (1997) 1488–1498.
[15] S.A. Lipton, Y.B. Choi, Z.H. Pan, et al., A redox-based mechanism for the neuroprotective and neurodestructive effects of nitric oxide and related nitroso-compounds, Nature 364 (1993) 626–632.
[16] M.B. Phillips, N.V. Povysheva, K.A. Harnett-Scott, E. Aizenman, J.W. Johnson. State-specific inhibition of NMDA receptors by memantine depends on intracellular calcium and provides insights into NMDAR channel blocker tolerability. bioRxiv. [preprint] doi.org/10.1101/2024.04.01.587624.
[17] W.E.G. Müller, H.C. Schröder, H. Ushijima, J. Dapper, J. Bormann, Gp120 of HIV-1 induces apoptosis in rat cortical cell cultures: Prevention by memantine, Eur. J. Pharm. 226 (1992) 209–214.
[18] W.E.G. Müller, G. Pergande, C. Schleger, H. Ushijima, S. Perović, Neurotoxicity in rat cortical cells caused by *N*-methyl-D-aspartate (NMDA) and Gp120 of HIV-1: Induction and pharmacological intervention, Progr. Molec Subcell. Biol. 16 (1996) 44–71.
[19] S.A. Lipton, Memantine prevents HIV coat protein-induced neuronal injury *in vitro*, Neurology 42 (1992) 1403–1405.
[20] M. Ge, J. Zhang, S. Chen, et al., Role of calcium homeostasis in Alzheimer's disease, Neuropsychiatr. Dis. Treat. 18 (2022) 487–498.
[21] S.V. Zaichick, K.M. McGrath, G. Caraveo, The role of Ca^{2+} signaling in Parkinson's disease, Dis. Model Mech. 10 (2017) 519–535.

[22] W.J. Goldberg, R.M. Kadingo, J.N. Barrett, Effects of ischemia-like conditions on cultured neurons: protection by low Na^+, low Ca^{2+} solutions, J. Neurosci. 6 (1986) 3144–3151.

[23] S. Eimerl, M. Schramm, The quantity of calcium that appears to induce neuronal death, J. Neurochem. 62 (1994) 1223–1226.

[24] M.J. Berridge, P. Lipp, M.D. Bootman, The versatility and universality of calcium signalling, Nat. Rev. Mol. Cell Biol. 1 (2000) 11–21.

[25] M. Maiolino, N. O'Neill, V. Lariccia, et al., Inorganic polyphosphate regulates AMPA and NMDA receptors and protects against glutamate excitotoxicity *via* activation of P2Y receptors, J. Neurosci. 39 (2019) 6038–6048.

[26] P. Dinarvand, S.M. Hassanian, S.H. Qureshi, et al., Polyphosphate amplifies proinflammatory responses of nuclear proteins through interaction with receptor for advanced glycation end products and P2Y1 purinergic receptor, Blood 123 (2014) 935–945.

[27] L. Tagliafico, M.E. Solesio, Could inorganic polyphosphate be a valid target against neuronal senescence? Neural Regen. Res 21 (2026) 1106–1107.

[28] G. López-Doménech, J.T. Kittler, Mitochondrial regulation of local supply of energy in neurons, Curr. Opin. Neurobiol. 81 (2023) 102747.

[29] M.A. DeTure, D.W. Dickson, The neuropathological diagnosis of Alzheimer's disease, Mol. Neurodegener. 14 (2019) 32.

[30] A. Alzheimer, Die Colloidentartung des Gehirns. [The colloidal degeneration of the brain], Arch. F. Psychiatr. U. Nervenkrankh. [Arch. Psychiatry Nerv. Dis.] 30 (1897) 18–53.

[31] N. Iwamoto, E. Nishiyama, J. Ohwada, H. Arai, Distribution of amyloid deposits in the cerebral white matter of the Alzheimer's disease brain: relationship to blood vessels, Acta Neuropathol. 93 (1997) 334–340.

[32] R.J. O'Brien, P.C. Wong, Amyloid precursor protein processing and Alzheimer's disease, Annu Rev. Neurosci. 34 (2011) 185–204.

[33] G. Evin, Q.X. Li, Platelets and Alzheimer's disease: potential of APP as a biomarker, World J. Psychiatry 2 (2012) 102–113.

[34] H. Zhang, Q. Ma, Y.W. Zhang, H. Xu, Proteolytic processing of Alzheimer's β-amyloid precursor protein, J. Neurochem. 120 (1) (2012) 9–21.

[35] K. Ono, T. Watanabe-Nakayama, Aggregation and structure of amyloid β-protein, Neurochem. Int 151 (2021) 105208.

[36] H. Yang, J. Li, X. Li, et al., Based on molecular structures: Amyloid-β generation, clearance, toxicity and therapeutic strategies, Front Mol. Neurosci. 15 (2022) 927530.

[37] K. Taniguchi, F. Yamamoto, A. Amano, A. Tamaoka, N. Sanjo, T. Yokota, F. Kametani, W. Araki, Amyloid-β oligomers interact with NMDA receptors containing GluN2B subunits and metabotropic glutamate receptor 1 in primary cortical neurons: Relevance to the synapse pathology of Alzheimer's disease, Neurosci. Res 180 (2022) 90–98.

[38] G. Mairet-Coello, J. Courchet, S. Pieraut, V. Courchet, A. Maximov, F. Polleux, The CAMKK2-AMPK kinase pathway mediates the synaptotoxic effects of Aβ oligomers through Tau phosphorylation, Neuron 78 (2013) 94–108.

[39] M. Naldi, J. Fiori, M. Pistolozzi, et al., Amyloid β-peptide 25-35 self-assembly and its inhibition: a model undecapeptide system to gain atomistic and secondary structure details of the Alzheimer's disease process and treatment, ACS Chem. Neurosci. 3 (2012) 952–962.

[40] I. Blasko, M. Wagner, N. Whitaker, B. Grubeck-Loebenstein, P. Jansen-Dürr, The amyloid β peptide aβ (25-35) induces apoptosis independent of p53, FEBS Lett. 470 (2000) 221–225.

[41] J.S. Mitchell, D.F. Hermens, M.R. Bennett, A.T. Can, J. Lagopoulos, Ketamine and zinc: treatment of anorexia nervosa *via* dual NMDA receptor modulation, CNS Drugs 37 (2023) 159–180.

[42] B.A. Yankner, T. Lu, Amyloid beta-protein toxicity and the pathogenesis of Alzheimer disease, J. Biol. Chem. 284 (2009) 4755–4759.

[43] B.A. Yankner, L.R. Dawes, S. Fisher, L. Villa-Komaroff, M.L. Oster-Granite, R. L. Neve, Neurotoxicity of a fragment of the amyloid precursor associated with Alzheimer's disease, Science 245 (1989) 417–420.

[44] J.Y. Koh, L.L. Yang, C.W. Cotman, β-amyloid protein increases the vulnerability of cultured cortical neurons to excitotoxic damage, Brain Res. 533 (1990) 315–320.

[45] D.T. Loo, A. Copani, C.J. Pike, E.R. Whittemore, A.J. Walencewicz, C.W. Cotman, Apoptosis is induced by β-amyloid in cultured central nervous system neurons, Proc. Natl. Acad. Sci. USA 90 (1993) 7951–7955.

[46] W.E.G. Müller, F.J. Romero, S. Perović, G. Pergande, P. Pialoglou, Protection of flupirtine on ß-amyloid-induced apoptosis in neuronal cells in vitro. Prevention of amyloid-induced glutathione depletion, J. Neurochem. 68 (1997) 2371–2377.

[47] I. Canobbio, Blood platelets: Circulating mirrors of neurons? Res Pr. Thromb. Haemost. 3 (2019) 564–565.

[48] P.M. Suess, S.A. Smith, J.H. Morrissey, Platelet polyphosphate induces fibroblast chemotaxis and myofibroblast differentiation, J. Thromb. Haemost. 18 (2020) 3043–3052.

[49] W.E.G. Müller, M. Neufurth, S.F. Wang, H.C. Schröder, X.H. Wang, Polyphosphate nanoparticles: balancing energy requirements in tissue regeneration processes, Small 20 (2024) 2309528.

[50] H. Schepler, M. Neufurth, S.F. Wang, et al., Acceleration of chronic wound healing by bio-inorganic polyphosphate: *In vitro* studies and first clinical applications, Theranostics 12 (2022) 18–34.

[51] W.E.G. Müller, H. Schepler, M. Neufurth, et al., The physiological polyphosphate as a healing biomaterial for chronic wounds: Crucial roles of its antibacterial and unique metabolic energy supplying properties, J. Mat. Sci. Technol. 135 (2023) 170–185.

[52] A.Y. Baev, P.R. Angelova, A.Y. Abramov, Inorganic polyphosphate is produced and hydrolyzed in F_0F_1-ATP synthase of mammalian mitochondria, Biochem J. 477 (2020) 1515–1524.

[53] W.E.G. Müller, H.C. Schröder, X.H. Wang, Inorganic polyphosphates as storage for and generator of metabolic energy in the extracellular matrix, Chem. Rev. 119 (2019) 12337–12374.

[54] F.A. Ruiz, C.R. Lea, E. Oldfield, R. Docampo, Human platelet dense granules contain polyphosphate and are similar to acidocalcisomes of bacteria and unicellular eukaryotes, J. Biol. Chem. 279 (2004) 44250–44257.

[55] J.I. Weitz, J.C. Fredenburgh, Platelet polyphosphate: the long and the short of it, Blood 129 (2017) 1574–1575.

[56] J.J. Verhoef, A.D. Barendrecht, K.F. Nickel, et al., Polyphosphate nanoparticles on the platelet surface trigger contact system activation, Blood 129 (2017) 1707–1717.

[57] W.E.G. Müller, S.F. Wang, E. Tolba, et al., Transformation of amorphous polyphosphate nanoparticles into coacervate complexes: an approach for the encapsulation of mesenchymal stem cells, Small 14 (2018) e1801170.

[58] W.E.G. Müller, M. Neufurth, I. Lieberwirth, S.F. Wang, H.C. Schröder, X.H. Wang, Functional importance of coacervation to convert calcium polyphosphate nanoparticles into the physiologically active state, Mater. Today Bio 16 (2022) 100404.

[59] M.S. Wolfe, Inhibition and modulation of gamma-secretase for Alzheimer's disease, Neurotherapeutics 5 (2008) 391–398.

[60] C.M. Cremers, D. Knoefler, S. Gates, et al., Polyphosphate: a conserved modifier of amyloidogenic processes, Mol. Cell 63 (2016) 768–780.

[61] M. Forsberg, H. Seth, A. Björefeldt, et al., Ionized calcium in human cerebrospinal fluid and its influence on intrinsic and synaptic excitability of hippocampal pyramidal neurons in the rat, J. Neurochem. 149 (2019) 452–470.

[62] X. Chen, D. Moore-Nichols, H. Nguyen, E.K. Michaelis, Calcium influx through NMDA receptors, chronic receptor inhibition by ethanol and 2-amino-5-phospho-nopentanoic acid, and receptor protein expression, J. Neurochem. 72 (1999) 1969–1980.

[63] W.E.G. Müller, S.F. Wang, M. Ackermann, et al., Rebalancing β-amyloid-induced decrease of ATP level by amorphous nano/micro polyphosphate: Suppression of the neurotoxic effect of amyloid β-protein fragment 25-35, Int J. Mol. Sci. 18 (2017) 2154.

[64] B.R. Ransom, E. Neale, M. Henkart, P.N. Bullock, P.G. Nelson, Mouse spinal cord in cell culture. I. Morphology and intrinsic neuronal electrophysiologic properties, J. Neurophysiol. 40 (1977) 1132–1150.

[65] E. Bondy-Chorney, I. Abramchuk, R. Nasser, et al., A broad response to intracellular long-chain polyphosphate in human cells, Cell Rep. 33 (2020) 108318.

[66] A. Lalatsa, A.M. Butt, Physiology of the blood brain barrier and mechanisms of transport across the blood brain barrier, in: P. Kesharwani, U. Gupta (Eds.), Nanotechnology-Based Targeted Drug Delivery Systems for Brain Tumors, 1st ed, Academic Press, 2018, pp. 49–66.

[67] W. Gong, Z. Wang, N. Liu, et al., Improving efficiency of adriamycin crossing blood brain barrier by combination of thermosensitive liposomes and hyperthermia, Biol. Pharm. Bull. 34 (2011) 1058–1064.

[68] J. Nong, P.M. Glassman, V.V. Shuvaev, et al., Targeting lipid nanoparticles to the blood-brain barrier to ameliorate acute ischemic stroke, Mol. Ther. 32 (2024) 1344–1358.

[69] M. Agrawal, S. Saraf, S. Saraf, et al., Stimuli-responsive *in situ* gelling system for nose-to-brain drug delivery, J. Control Release 327 (2020) 235–265.

[70] J.T. Trevino, R.C. Quispe, F. Khan, V. Novak, Non-invasive strategies for nose-to-brain drug delivery, J. Clin. Trials 10 (2020) 439.

[71] L.F. Hassan, R. Sen, T.M. O'Shea, Trehalose-based coacervates for local bioactive protein delivery to the central nervous system, Biomaterials 309 (2024) 122594.

[72] W.E.G. Müller, E. Tolba, H.C. Schröder, et al., A new polyphosphate calcium material with morphogenetic activity, Mater. Lett. 148 (2015) 163–166.

[73] C.J. Barrow, A. Yasuda, P.T. Kenny, M.G. Zagorski, Solution conformations and aggregational properties of synthetic amyloid beta-peptides of Alzheimer's disease, Anal. Circ. dichroism Spectra J. Mol. Biol. 225 (1992) 1075–1093.

[74] B. Lorenz, S. Marmé, W.E.G. Müller, K. Unger, H.C. Schröder, Preparation and use of polyphosphate-modified zirconia for purification of nucleic acids and proteins, Anal. Biochem 216 (1994) 118–126.

[75] E.F. Pettersen, T.D. Goddard, C.C. Huang, et al., UCSF Chimera–a visualization system for exploratory research and analysis, J. Comput. Chem. 25 (2004) 1605–1612.

[76] A. Chattopadhyay, R. Rukmini, S. Mukherjee, Photophysics of a neurotransmitter: ionization and spectroscopic properties of serotonin, Biophys. J. 71 (1996) 1952–1960.

[77] S. Nag, J. Balaji, P.K. Madhu, S. Maiti, Intermolecular association provides specific optical and NMR signatures for serotonin at intravesicular concentrations, Biophys. J. 94 (2008) 4145–4153.

[78] E.Y. Yuen, Q. Jiang, P. Chen, Z. Gu, J. Feng, Z. Yan, Serotonin 5-HT1A receptors regulate NMDA receptor channels through a microtubule-dependent mechanism, J. Neurosci. 25 (2005) 5488–5501.

[79] S. Perovic, C. Schleger, G. Pergande, et al., The triaminopyridine flupirtine prevents cell death in rat cortical cells induced by N-methyl-D-aspartate and gp120 of HIV-1, Eur. J. Pharm. 288 (1994) 27–33.

[80] N. Bansal, A. Houle, G. Melnykovych, Apoptosis: mode of cell death induced in T cell leukemia lines by dexamethasone and other agents, FASEB J. 5 (1991) 211–216.

[81.] H. Ushijima, S. Perović, J. Leuck, P.G. Rytik, W.E.G. Müller, H.C. Schröder, Suppression of PrP^{Sc}- and HIV-1 gp120 induced neuronal cell death by sulfated colomic acid, J. NeurVirol. 5 (1999) 289–299.

[82] G. Grynkiewicz, M. Poenie, R.Y. Tsien, A new generation of Ca^{2+} indicators with greatly improved fluorescence properties, J. Biol. Chem. 260 (1985) 3440–3450.

[83] M. Kawahara, Y. Kuroda, Intracellular calcium changes in neuronal cells induced by Alzheimer's beta-amyloid protein are blocked by estradiol and cholesterol, Cell Mol. Neurobiol. 21 (2001) 1–13.

[84] E. Caballero, E. Hernando-Pérez, V. Tapias, M. Calvo-Rodríguez, C. Villalobos, L. Núñez, Amyloid beta oligomers-induced Ca^{2+} entry pathways: role of neuronal networks, NMDA receptors and amyloid channel formation, Biomedicines 10 (2022) 1153.

[85] A. Aiello, E. Fattorusso, A. Giordano, et al., Damipipecolin and damituricin, novel bioactive bromopyrrole alkaloids from the Mediterranean sponge *Axinella damicornis*, Bioorg. Med Chem. 15 (2007) 5877–5887.

[86] O.L. Barreto-Chang, R.E. Dolmetsch, Calcium imaging of cortical neurons using Fura-2 AM, J. Vis. Exp. 19 (2009) 1067.

[87] M. Abbas, W.P. Lipiński, J. Wang, E. Spruijt, Peptide-based coacervates as biomimetic protocells, Chem. Soc. Rev. 50 (2021) 3690–3705.

[88] S.F. Wang, M. Neufurth, H. Schepler, et al., Liquid-liquid phase transition as basis for novel materials for skin repair and regeneration, J. Mater. Chem. B 12 (2024) 96224–99638.

[89] J. Kreuter, R.N. Alyautdin, D.A. Kharkevich, A.A. Ivanov, Passage of peptides through the blood-brain barrier with colloidal polymer particles (nanoparticles), Brain Res. 674 (1995) 171–174.

[90] T.M. Nalawade, K. Bhat, S.H. Sogi, Bactericidal activity of propylene glycol, glycerine, polyethylene glycol 400, and polyethylene glycol 1000 against selected microorganisms, J. Int Soc. Prev. Community Dent. 5 (2015) 114–119.

[91] W.E.G. Müller, H.C. Schröder, M. Neufurth, X.H. Wang, An unexpected biomaterial against SARS-CoV-2: Bio-polyphosphate blocks binding of the viral spike to the cell receptor, Mater. Today 51 (2021) 504–524.

[92] M. Trenkel, R. Scherließ, Nasal powder formulations: *In-vitro* characterisation of the impact of powders on nasal residence time and sensory effects, Pharmaceutics 13 (2021) 385.

[93] J.J. Christ, S. Willbold, L.M. Blank, Methods for the analysis of polyphosphate in the life sciences, Anal. Chem. 92 (2020) 4167–4176.

[94] M. Kokkinopoulou, M.A. Güler, B. Lieb, M. Barbeck, S. Ghanaati, J. Markl, 3D-ultrastructure, functions and stress responses of gastropod (Biomphalaria glabrata) rhogocytes, PLoS ONE 9 (2014) e101078.

[95] A. Petrie, P. Watson, eds. Statistics for Veterinary and Animal Science, 3rd ed. Oxford; 2013:85-99.

[96] D. Gate, N. Saligrama, O. Leventhal, et al., Clonally expanded CD8 T cells patrol the cerebrospinal fluid in Alzheimer's disease, Nature 577 (2020) 399–404.

[97] C. Curtis, D. Toghani, B. Wong, E. Nance, Colloidal stability as a determinant of nanoparticle behavior in the brain, Colloids Surf. B Biointerfaces 170 (2018) 673–682.

[98] T. Burnouf, T.L. Walker, The multifaceted role of platelets in mediating brain function, Blood 140 (2022) 815–827.

[99] F. Gaertner, S. Massberg, Patrolling the vascular borders: platelets in immunity to infection and cancer, Nat. Rev. Immunol. 19 (2019) 747–760.

[100] G. Marcoux, A. Laroche, J. Espinoza Romero, E. Boilard, Role of platelets and megakaryocytes in adaptive immunity, Platelets 32 (2021) 340–351.

[101] M.J. Page, E. Pretorius, Platelet behavior contributes to neuropathologies: a focus on Alzheimer's and Parkinson's disease, Semin Thromb. Hemost. 48 (2021) 382–404.

[102] A. Sato, H. Aizawa, T. Tsujino, et al., Fluorescent cytochemical detection of polyphosphates associated with human platelets, Int J. Mol. Sci. 22 (2021) 1040.

[103] B. Lorenz, J. Münkner, M.P. Oliveira, et al., Changes in metabolism of inorganic polyphosphate in rat tissues and human cells during development and apoptosis, Biochim Biophys. Acta 1335 (1997) 51–60.

[104] E.C. Toescu, Apoptosis and cell death in neuronal cells: where does Ca^{2+} fit in? Cell Calcium 24 (1998) 387–403.

[105] D. Wu, Q. Chen, X. Chen, F. Han, Z. Chen, Y. Wang, The blood-brain barrier: structure, regulation, and drug delivery, Signal Transduct. Target Ther. 8 (2023) 217.

[106] A. Silvin, J. Qian, F. Ginhoux, Brain macrophage development, diversity and dysregulation in health and disease, Cell Mol. Immunol. 20 (2023) 1277–1289.

[107] H. Schepler, X.H. Wang, M. Neufurth, S.F. Wang, H.C. Schröder, W.E.G. Müller, The therapeutic potential of inorganic polyphosphate: a versatile physiological polymer to control coronavirus disease (COVID-19), Theranostics 11 (2021) 6193–6213.

[108] R. Taléns-Visconti, J.V. de Julián-Ortiz, O. Vila-Busó, O. Diez-Sales, A. Nácher, Intranasal drug administration in Alzheimer-type dementia: towards clinical applications, Pharmaceutics 15 (2023) 1399.

[109] H.M. van der Kooij, E. Spruijt, I.K. Voets, R. Fokkink, M.A. Cohen Stuart, J. van der Gucht, On the stability and morphology of complex coacervate core micelles: from spherical to wormlike micelles, Langmuir 28 (2012) 14180–14191.

[110] L. Godfrey, A. Iannitelli, N.L. Garrett, et al., Nanoparticulate peptide delivery exclusively to the brain produces tolerance free analgesia, J. Control Release 270 (2018) 135–144.

[111] FDA/PMA. Tissue adhesive for use in embolization of brain arteriovenous malformations. Accessed 20 October 2000. ⟨https://www.accessdata.fda.gov/scripts/cdrh/cfdocs/cfpma/pma.cfm?id=p990040⟩.

[112] E. Pavlov, R. Aschar-Sobbi, M. Campanella, R.J. Turner, M.R. Gómez-García, A. Y. Abramov, Inorganic polyphosphate and energy metabolism in mammalian cells, J. Biol. Chem. 285 (2010) 9420–9428.

[113] B. McIntyre, M.E. Solesio, Mitochondrial inorganic polyphosphate (polyP): the missing link of mammalian bioenergetics, Neural Regen. Res 16 (2021) 2227–2228.

[114] R.T. Da Costa, A. Nichenko, M.M. Perez, et al., Mammalian mitochondrial inorganic polyphosphate (polyP) and cell signaling: crosstalk between polyP and the activity of AMPK, Mol. Metab. 91 (2025) 102077.

[115] C. Schoenichen, C. Bode, D. Duerschmied, Role of platelet serotonin in innate immune cell recruitment, Front Biosci. 24 (2019) 514–526.

[116] U. Lalo, Y. Pankratov, ATP-mediated signalling in the central synapses, Neuropharmacology 229 (2023) 109477.

[117] W.E.G. Müller, P. Pialoglou, F.J. Romero, S. Perović, G. Pergande, Protective effect of the drug flupirtine on ß-amyloid-induced apoptosis in primary neuronal cells *in vitro*. In: proceedings of the fifth international conference on Alzheimer's disease and related disorders, Neurobiol. Aging (1996) S152.

[118] B. Wiatrak, P. Mieszała, K. Gąsiorowski, Impact of NMDA receptor activation on DNA damage in PC12 neuron-like cell cultures in the presence of β-amyloid peptides, Mol. Biol. Rep. 49 (2022) 10443–10455.

[119] A.Y. Abramov, M.R. Duchen, Impaired mitochondrial bioenergetics determines glutamate-induced delayed calcium deregulation in neurons, Biochim Biophys. Acta 1800 (2010) 297–304.

[120] W.E.G. Müller, F.J. Romero, S. Perović, G. Pergande, P. Pialoglou, Protective effect of the drug Flupirtine on ß-amyloid-induced apoptosis in primary neuronal cells *in vitro*, J. Brain Res. 37 (1996) 575–577.

[121] S.C. Stotz, L.O. Scott, C. Drummond-Main, et al., Inorganic polyphosphate regulates neuronal excitability through modulation of voltage-gated channels, Mol. Brain 7 (2014) 42.

[122] M. Tymianski, M.C. Wallace, I. Spigelman, et al., Cell-permeant Ca^{2+} chelators reduce early excitotoxic and ischemic neuronal injury *in vitro* and *in vivo*, Neuron 11 (1993) 221–235.

[123] H.A. Scheidt, A. Korn, B. Schwarze, M. Krueger, D. Huster, Conformation of Pyroglutamated Amyloid β (3-40) and (11-40) Fibrils - extended or Hairpin? J. Phys. Chem. B 128 (2024) 1647–1655.

[124] P. Garcés, A. Amaro, M. Montecino, B. van Zundert, Inorganic polyphosphate: from basic research to diagnostic and therapeutic opportunities in ALS/FTD, Biochem Soc. Trans. 52 (2024) 123–135.

[125] A.Y. Abramov, C. Fraley, C.T. Diao, et al., Targeted polyphosphatase expression alters mitochondrial metabolism and inhibits calcium-dependent cell death, Proc. Natl. Acad. Sci. USA 104 (2007) 18091–18096.

[126] M.E. Solesio, L.C. Garcia Del Molino, P.A. Elustondo, C. Diao, J.C. Chang, E. V. Pavlov, Inorganic polyphosphate is required for sustained free mitochondrial calcium elevation, following calcium uptake, Cell Calcium 86 (2020) 102127.

[127] K.M. Holmström, N. Marina, A.Y. Baev, N.W. Wood, A.V. Gourine, A.Y. Abramov, Signalling properties of inorganic polyphosphate in the mammalian brain, Nat. Commun. 4 (2013) 1362.

[128] P.R. Angelova, K.Z. Iversen, A.G. Teschemacher, S. Kasparov, A.V. Gourine, A. Y. Abramov, Signal transduction in astrocytes: Localization and release of inorganic polyphosphate, Glia 66 (2018) 2126–2136.

[129] A. Kornberg, N.N. Rao, D. Ault-Riché, Inorganic polyphosphate: a molecule of many functions, Annu Rev. Biochem 68 (1999) 89–125.

[130] R.K.W. Mailer, L. Hänel, M. Allende, T. Renné, Polyphosphate as a target for interference with inflammation and thrombosis, Front. Med. 6 (2019) 76.

[131] K.D. Kumble, A. Kornberg, Inorganic polyphosphate in mammalian cells and tissues, J. Biol. Chem. 270 (1995) 5818–5822.

[132] S.A. Smith, N.J. Mutch, D. Baskar, P. Rohloff, R. Docampo, J.H. Morrissey, Polyphosphate modulates blood coagulation and fibrinolysis, Proc. Natl. Acad. Sci. USA 103 (2006) 903–908.

[133] H. Demirin, H. Ozhan, T. Ucgun, et al., Normal range of mean platelet volume in healthy subjects: Insight from a large epidemiologic study, Thromb. Res 128 (2011) 358–360.

[134] H. Holmsen, H.J. Weiss, Further evidence for a deficient storage pool of adenine nucleotides in platelets from some patients with thrombocytopathia–"storage pool disease", Blood 39 (1972) 197–209.

[135] H. Holmsen, H.J. Weiss, Secretable storage pools in platelets, Annu Rev. Med 30 (1979) 119–134.

[136] E.A. Bonnin, A. Golmohammadi, R. Rehm, C. Tetzlaff, S.O. Rizzoli, High-resolution analysis of bound Ca^{2+} in neurons and synapses, Life Sci. Alliance 7 (2023) e202302030.

[137] P.W. Andrews, C. Bosyj, L. Brenton, et al., All the brain's a stage for serotonin: the forgotten story of serotonin diffusion across cell membranes, Proc. Biol. Sci. 289 (2022) 20221565.

[138] R. Omidyan, Z. Amanollahi, G. Azimi, Protonated serotonin: Geometry, electronic structures and photophysical properties, Spectrochim. Acta A Mol. Biomol. Spectrosc. 182 (2017) 8–16.

[139] J.L. Fitch-Tewfik, R. Flaumenhaft, Platelet granule exocytosis: a comparison with chromaffin cells, Front Endocrinol. (Lausanne) 4 (2013) 77.

[140] G. Raposo, M.S. Marks, Melanosomes–dark organelles enlighten endosomal membrane transport, Nat. Rev. Mol. Cell Biol. 8 (2007) 786–797.

[141] M.S. Marks, H.F. Heijnen, G. Raposo, Lysosome-related organelles: unusual compartments become mainstream, Curr. Opin. Cell Biol. 25 (2013) 495–505.

[142] A. Dupuis, J.C. Bordet, A. Eckly, C. Gachet, Platelet δ-storage pool disease: an update, J. Clin. Med 9 (2020) 2508.

[143] K.K. Nakashima, M.A. Vibhute, E. Spruijt, Biomolecular chemistry in liquid phase separated compartments, Front Mol. Biosci. 6 (2019) 21.

[144] H.C. Schröder, M. Neufurth, H. Zhou, S.F. Wang, X.H. Wang, W.E.G. Müller, Inorganic polyphosphate: Coacervate formation and functional significance in nanomedical applications, Int J. Nanomed. 17 (2022) 5825–5850.

[145] J. Kreuter, Nanoparticles and microparticles for drug and vaccine delivery, J. Anat. 189 (Pt 3) (1996) 503–505.

[146] R.N. Aliautdin, V.E. Petrov, A.A. Ivanov, J. Kreuter, D.A. Kharkevich, Transport of the hexapeptide dalargin across the hemato-encephalic barrier into the brain using polymer nanoparticles, Eksp. Klin. Farm. 59 (1996) 57–60.
[147] J. Kreuter, Nanoparticulate systems for brain delivery of drugs, Adv. Drug Deliv. Rev. 47 (2001) 65–81.
[148] T.P. Crowe, M.H.W. Greenlee, A.G. Kanthasamy, W.H. Hsu, Mechanism of intranasal drug delivery directly to the brain, Life Sci. 195 (2018) 44–52.
[149] G. Cárdenas, G. Fragoso, E. Sciutto, Neuroinflammation in severe acute respiratory syndrome Coronavirus-2 (SARS-CoV-2) infection: pathogenesis and clinical manifestations, Curr. Opin. Pharm. 63 (2022) 102181.
[150] B.A. Aderibigbe, *In situ*-based gels for nose to brain delivery for the treatment of neurological diseases, Pharmaceutics 10 (2018) 40.
[151] Y. Qiu, S.K. Hamilton, J. Temenoff, Improving mechanical properties of injectable polymers and composites, in: B. Vernon (Ed.), Injectable Biomaterials, Woodhead Publishing, 2011, pp. 61–91.
[152] M. Dholakia, V. Thakkar, N. Patel, T. Gandhi, Development and characterisation of thermo-reversible mucoadhesive moxifloxacin hydrochloride in situ ophthalmic gel, J. Pharm. Bioallied Sci. 4 (1) (2012) S42–S45.
[153] C. Arredondo, C. Cefaliello, A. Dyrda, et al., Excessive release of inorganic polyphosphate by ALS/FTD astrocytes causes non-cell-autonomous toxicity to motoneurons, Neuron 110 (2022) 1656–1670.e12.
[154] M. Brini, E. Carafoli, The plasma membrane Ca^{2+} ATPase and the plasma membrane sodium calcium exchanger cooperate in the regulation of cell calcium, Cold Spring Harb. Perspect. Biol. 3 (2011) a004168.
[155] C. Romei, M. Raiteri, L. Raiteri, GABA transporters mediate glycine release from cerebellum nerve endings: roles of Ca^{2+} channels, mitochondrial Na^{+}/Ca^{2+} exchangers, vesicular GABA/glycine transporters and anion channels, Neurochem. Int 61 (2012) 133–140.
[156] M. Brini, T. Calì, D. Ottolini, E. Carafoli, Neuronal calcium signaling: function and dysfunction, Cell Mol. Life Sci. 71 (2014) 2787–27814.
[157] T. Calì, R. Lopreiato, J. Shimony, et al., A novel mutation in isoform 3 of the plasma membrane Ca^{2+} pump impairs cellular Ca^{2+} homeostasis in a patient with cerebellar ataxia and laminin subunit 1α mutations, J. Biol. Chem. 290 (2015) 16132–16141.
[158] M. Dittrich, A.E. Homan, S.D. Meriney, Presynaptic mechanisms controlling calcium-triggered transmitter release at the neuromuscular junction, Curr. Opin. Physiol. 4 (2018) 15–24.
[159] I. Mody, MacDonald JF. NMDA receptor-dependent excitotoxicity: the role of intracellular Ca^{2+} release, Trends Pharm. Sci. 16 (1995) 356–359.
[160] J. Lempart, U. Jakob, Role of polyphosphate in amyloidogenic processes, Cold Spring Harb. Perspect. Biol. 11 (2019) a034041.
[161] R. Schmidt, U. Strähle, S. Scholpp, Neurogenesis in zebrafish - from embryo to adult, Neural Dev. 8 (2013) 3.
[162] M. Neufurth, H. Nassabi, S. Perovic-Ottstadt, R. Dobmeyer, R. Muñoz-Espí, H. Ushijima, H.C. Schröder, C. Wu, X.H. Wang, W.E.G. Müller, Unpublished results, Sodium polyphosphate, a new drug for treatment of atopic dermatitis: Basic considerations and clinical applications.